Electronic Supplementary Information

Narcissistic self-sorting in anion-coordination-driven assemblies

Xiaotong Zhao,[a] Heng Wang,[b] Boyang Li,[a] Bo Zheng,[a] Dong Yang,[a] Wenhua Xu,[a] Xiaopeng Li,[b] Xiao-Juan Yang,[a] Biao Wu*[a]

[a] *Key Laboratory of Synthetic and Natural Functional Molecule Chemistry of the Ministry of Education, College of Chemistry and Materials Science, Northwest University, Xi'an 710069, China*

[b] *College of Chemistry and Environmental Engineering, Shenzhen University, Shenzhen 518055, China*

E-mail: wubiao@nwu.edu.cn

Table of Contents:

S1. General considerations.

2-Nitrophenyl isocyanate and 4-nitrophenyl isocyanate were purchased from Alfa Aesar and used as received. $(TBA)_2SO_4$ were purchased from Alfa Aesar and diluted the 50% water solution to 0.625 mol/L water solution. All solvents and other reagents were of reagent grade quality. All ^{1}H NMR, COSY and DOSY spectra were obtained at 300 K by using Bruker AVANCE III-400 MHz spectrometers; ^{13}C NMR spectra were obtained at 300 K by using Bruker AVANCE III-400 MHz spectrometers and JEOL RESONANCE ECZ600R; ^{1}H and ^{13}C NMR chemical shifts were reported relative to residual solvent peaks (^{1}H NMR: 2.50 ppm for DMSO-d_6; ^{13}C NMR: 39.52 for DMSO-d_6). ESI-MS measurements were carried out using a Bruker micro TOF-Q II ESI-Q-TOF LC/MS/MS spectrometer and Waters Synapt-G2.

S2. Synthesis of the ligands.

S2.1 Synthesis of ligand L^1

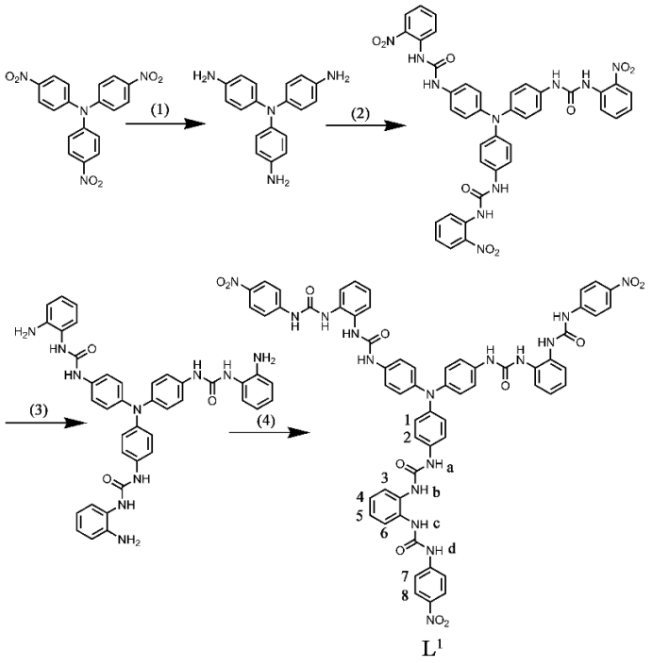

Scheme S1. Synthesis of the ligand $\mathbf{L^1}$: (1) and (3) $NH_2NH_2 \cdot H_2O$, Pd/C 10% cat., EtOH; (2) 2-nitrophenylisocyanate, THF; (4) 4-nitrophenylisocyanate, THF/DMF.

Ligand L^1

$\mathbf{L^1}$ was prepared according to reported literature procedures.[1] ^{1}H NMR (400 MHz,DMSO-d_6, ppm): δ 9.84 (s, 3H, NHd), 8.99 (s, 3H, NHc), 8.26 (s, 3H, NHb), 8.18 (d, J = 9.2 Hz, 6H, H8), 8.05 (s, 3H, NHa), 7.70 (d, J = 9.2 Hz, 2H, H7), 7.64 (d, J = 8.0 Hz, 1H, H6), 7.53 (d, J = 8.0 Hz, 1H, H3), 7.36 (d, J = 8.8 Hz, 2H, H2), 7.12 (m, 2H, H4/5), 6.89 (d, J = 8.8 Hz, 2H, H1).

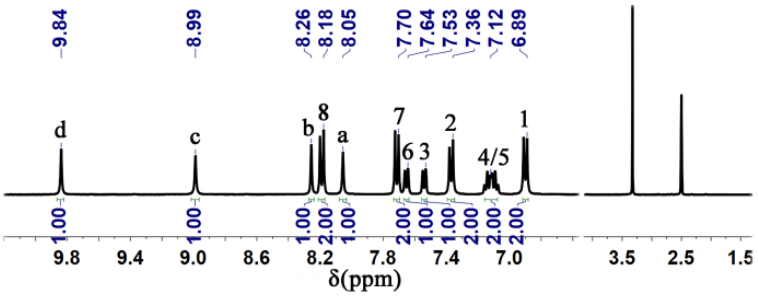

Fig. S1. ^{1}H NMR spectrum of $\mathbf{L^1}$ (400 MHz, DMSO-d_6, 300 K).

S2.2 Synthesis of ligand L^2

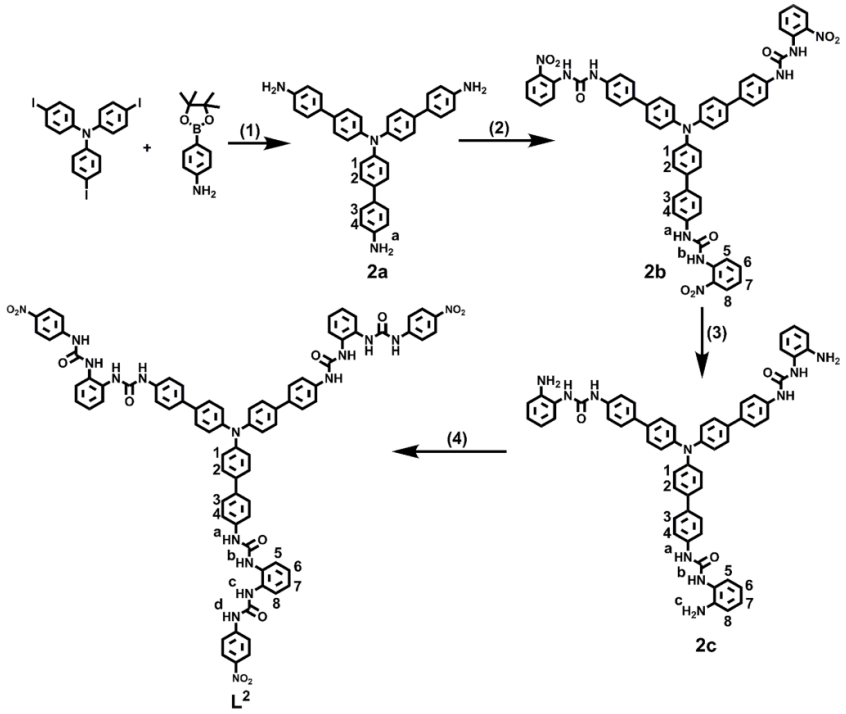

Scheme S2. Synthesis of ligand $\mathbf{L^2}$: (1) K_2CO_3, Pd(0), dioxane/H_2O; (2) 2-nitrophenyl isocyanate, THF; (3) NH_2NH_2 ·H_2O, Pd/C 10% cat., EtOH; (4) 4-nitrophenyl isocyanate, THF.

Compound 2a:

Tris(4-iodophenyl)amine (0.5 g, 0.8 mmol), 4-Aminophenylboronic acid pinacol ester (0.7 mg, 3.1 mmol), potassium carbonate (460 mg), and tetrakis(triphenylphosphine)palladium (50 mg) were added in dioxane (22.5 mL) under an inert atmosphere. After refluxing under intense stirring for 12 h, the solid was filtered through celite, and the solution was purified over a column of silica gel by eluting with CH_2Cl_2/MeOH (100:1 v/v). White compound **2a** was obtained by solvent evaporation (yield: 300 mg, 72%). ^{1}H NMR (400 MHz, DMSO-d_6, ppm): δ 7.46 (d, J = 8.8 Hz, 1H, H2), 7.32 (s, J = 8.4 Hz,1H, H3), 7.03 (d, J = 8.8 Hz, 1H, H1), 6.61 (d, J = 8.4 Hz，1H, H4), 5.18 (s, 2H, Ha). ^{13}C NMR (100 MHz, DMSO-d_6, ppm): 153.2(C), 150.3(C), 140.38(C), 132.4(C), 132.0(CH), 131.5(CH), 129.13(CH), 119.5(CH).

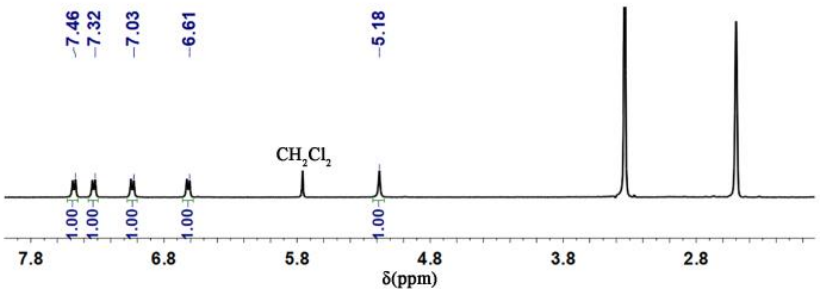

Fig. S2. ^{1}H NMR spectrum of compound **2a** (400 MHz, DMSO-d_6, 300 K)

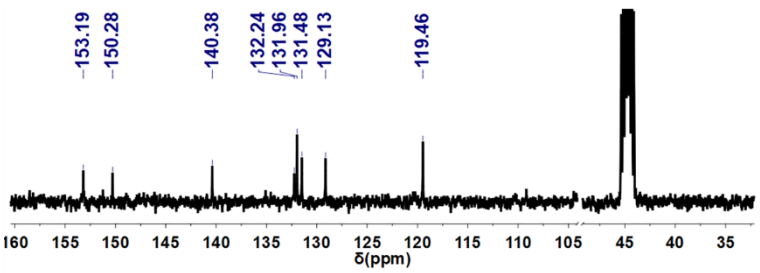

Fig. S3. ^{13}C NMR spectrum of **2a** (100 MHz, DMSO-d_6, 300 K).

Compound 2b:

Compound **2a** (0.35 g, 0.65 mmol) was dissolved in THF (15 mL) and was added to a THF (15 mL) solution of 2-nitro-phenylisocyanate (0.33 g, 2.0 mmol). After stirring overnight, the solvent was removed under reduced pressure, and the residue was washed several times with diethyl ether. It was then dried to yield analytically pure **2b** as a yellow solid (0.45 g, 0.44 mmol, 66%). ^{1}H NMR (400 MHz, DMSO-d_6, ppm): δ 9.94 (s, 1H, Hb), 9.63 (s, 1H, Ha), 8.30 (d, J = 8.4 Hz, 1H, H8), 8.10 (d, J = 8.4 Hz, 1H, H5), 7.72 (m, 1H, H6), 7.63 (d, J = 8.8 Hz, 4H, H2/3), 7.59 (d, J = 8.8 Hz, 2H, H1), 7.22 (m, 1H, H7), 7.14 (d, J = 8.8 Hz, 2H, H4). ^{13}C NMR (100 MHz, DMSO-d_6, ppm): δ 157.1 (CO), 151.1 (C), 143.6 (C), 142.8 (C), 140.2 (C), 140.1 (C), 139.5 (C), 138.9 (CH), 132.4 (CH), 131.8 (CH), 130.6 (CH), 129.4 (CH), 127.8 (CH), 127.4 (CH), 124.2 (CH). ESI-MS: *m/z* 100.00%, 1011.35 $[M+H]^+$.

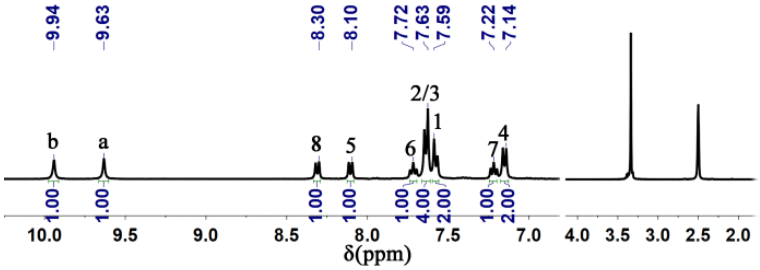

Fig. S4. ^{1}H NMR spectrum of **2b** (400 MHz, DMSO-d_6, 300 K).

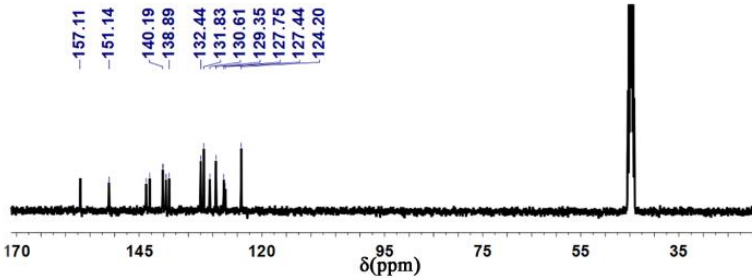

Fig. S5. ^{13}C NMR spectrum of **2b** (100 MHz, DMSO-d_6, 300 K).

Compound 2c:

Compound **2b** (0.30 g, 0.30 mmol) and Pd/C 10% (0.03 g, cat.) were mixed in ethanol (10 mL), and hydrazine monohydrate (10 mL) was added to this suspension. After heating at reflux with stirring overnight, the solid was filtered off via suction filtration and then dissolved in DMF (20 mL) and filtered

through celite to remove the Pd/C. The resulting DMF solution was poured into water (100 mL) to induce precipitation. The precipitate was collected and washed several times with ethanol and diethyl ether, then dried under vacuum to give **2c** as a white solid (0.23 g, 0.25 mmol, 84%). ^{1}H NMR (400 MHz, DMSO-d_6, ppm): δ 8.90 (s, 1H, Ha), 7.78 (s, 1H, Hb), 7.62 (m, 4H, H2/4), 7.55 (d, J = 8.4 Hz, 2H, H3), 7.37 (d, J = 8.0 Hz, 1H, H5), 7.16 (d, J = 8.8 Hz, 2H, H1), 6.86 (t, J = 8.0 Hz, 1H, H7), 6.77 (d, J = 8.0 Hz， 1H, H8), 6.59 (t, J = 8.0 Hz, 1H, H6), 4.79 (s, 2H, Hc). ^{13}C NMR (100 MHz, DMSO-d_6, ppm): δ 153.1 (CO), 145.8 (C), 140.9 (C), 139.3 (C), 134.5 (C), 132.7 (C), 127.1 (C), 126.5 (CH), 124.7 (CH), 124.4 (CH), 124.1 (CH), 123.78 (CH), 118.3 (CH), 116.8 (CH), 115.9 (CH). ESI-MS: m/z 100.00%, 943.40 [M+Na]$^{+}$.

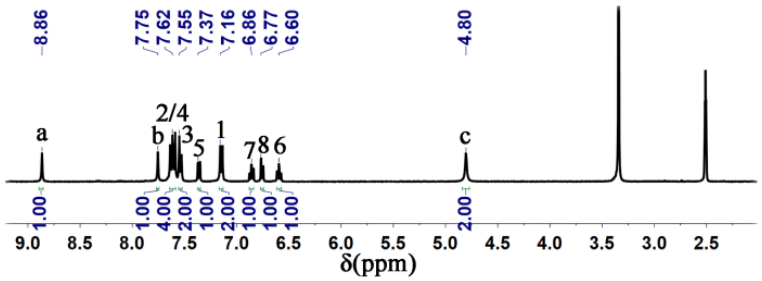

Fig. S6. ^{1}H NMR spectrum of compound **2c** (400 MHz, DMSO-d_6, 300 K).

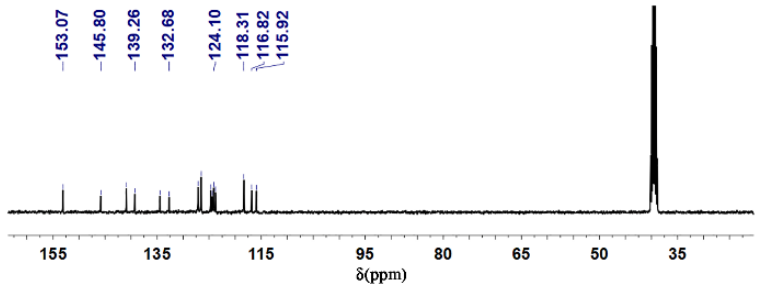

Fig. S7. ^{13}C NMR spectrum of **2c** (100 MHz, DMSO-d_6, 300 K).

Ligand L^{2}:

Compound **2c** (0.39 g, 0.42 mmol) was dissolved in 10 mL of DMF and the solution was added dropwise into a 10 mL THF solution of 4-nitro-phenylisocyanate (0.33 g, 2.0 mmol). The mixture was refluxed for 6 hours, then the solution was evaporated under reduced pressure to give a solid, which was washed several times with toluene and diethyl ether and then dried to get pure **L^{2}** as a gray solid (0.53 g, 0.37 mmol, 88%). ^{1}H NMR (400 MHz, DMSO-d_6, ppm): δ 9.87 (s, 1H, Ha), 9.18 (s, 1H, Hb), 8.29 (s, 1H, Hc), 8.18 (d, J = 8.8 Hz, 2H, H10), 8.14 (s, 1H, Hd), 7.73 (d, J = 8.8 Hz, 2H, H9), 7.59 (m, 8H, H1/2/3/4), 7.12 (m, 4H, H5/6/7/8). ^{13}C NMR (100 MHz, DMSO-d_6, ppm): δ 153.2 (CO), 152.8 (CO), 146.6 (C), 145.9 (C), 141.1 (C), 138.9 (C), 134.4 (C), 133.1 (C), 131.9 (C), 130.4 (C), 127.2 (CH), 126.6 (CH), 125.2 (CH), 124.8 (CH), 124.7 (CH), 124.1 (CH), 124.0 (CH), 123.8 (CH), 118.7 (CH), 117.4 (CH). ESI-MS: m/z 100.00%, 1435.47 [M+Na]$^{+}$.

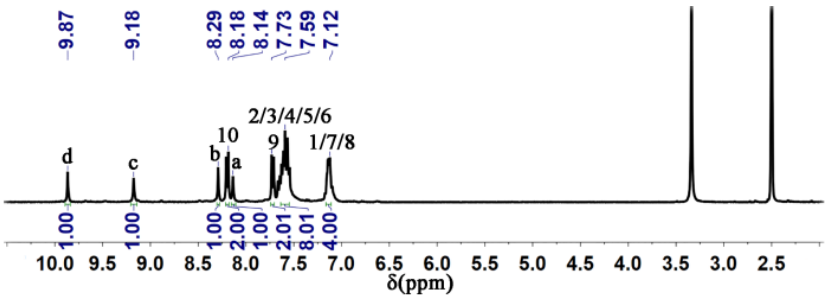

Fig. S8. ^{1}H NMR spectrum of **L**^{2} (400 MHz, DMSO-d_6, 300 K).

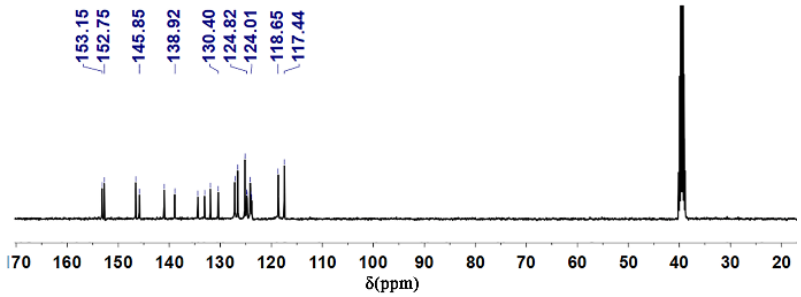

Fig. S9. ^{13}C NMR spectrum of **L**^{2} (100 MHz, DMSO-d_6, 300 K).

S2.3 Synthesis of ligand L^{3}

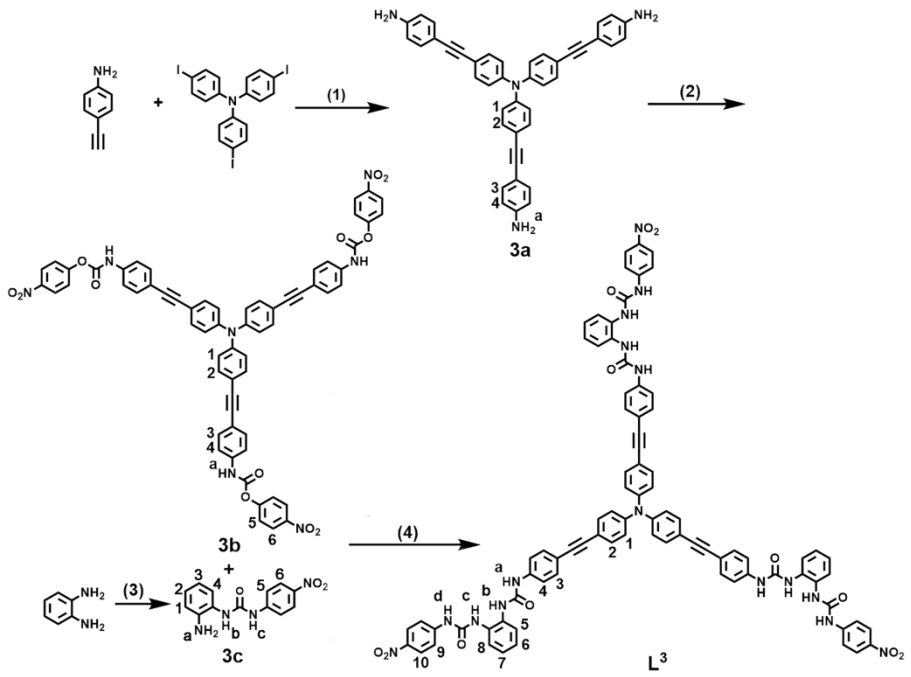

Scheme S3. Synthesis of ligand **L**^{3}: (1) $PdCl_2(PPh_3)_2$, CuI, DBU, rt; (2) 4-nitrophenyl chloroformate, THF; (3) 4-nitrophenyl isocyanate, THF. (4) Et_3N, DMF/THF, rt.

Compound 3a:

4-Ethynylbenzenamine (0.49 g, 4.2 mmol), tris(4-iodophenyl)amine (0.84 mg, 1.35 mmol), $PdCl_2(PPh_3)_2$ (0.02 g), CuI (0.006 g), and DBU (2.1 mL) were added to toluene (20 mL) under a nitrogen atmosphere. After stirring overnight at room temperature, the solution was purified over a column of silica gel, eluted with CH_2Cl_2. White product of compound **3a** was obtained by solvent evaporation (yield: 0.56 g, 0.95 mmol, 70%). ^{1}H NMR (400 MHz, DMSO-d_6, ppm): δ 7.41 (d, J = 8.0 Hz, 1H, H2), 7.16 (s, J = 8.0 Hz, 2H, H3), 7.00 (d, J = 8.0 Hz, 2H, H1), 6.54 (d, J = 8.0 Hz, 2H, H4), 5.54 (s, 2H, Ha). ^{13}C NMR (100 MHz, DMSO-d_6, ppm): δ 149.3 (C), 145.6 (C), 132.4 (C), 132.2 (C), 123.8 (CH), 118.1 (CH), 113.6 (CH), 108.3 (CH), 90.9 (C≡), 86.0 (C≡).

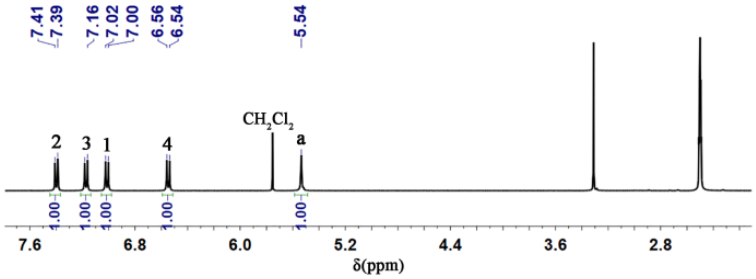

Fig. S10. ^{1}H NMR spectrum of **3a** (400 MHz, DMSO-d_6, 300 K).

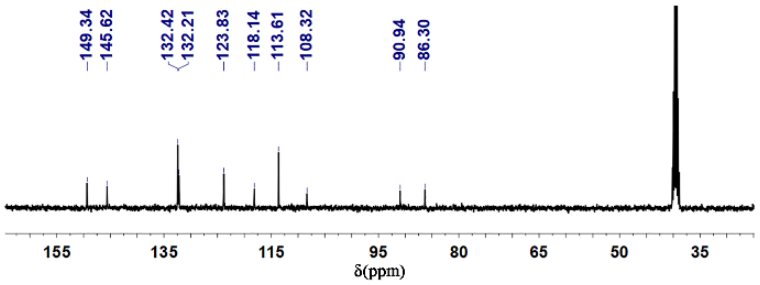

Fig. S11. ^{13}C NMR spectrum of **3a** (100 MHz, DMSO-d_6, 300 K).

Compound 3b:

Compound **3a** (118 mg, 0.2 mmol) was dissolved in THF (10 mL) and added dropwise to a solution of 4-nitrophenyl chloroformate (141 mg, 0.7 mmol) in THF (10 mL). After refluxed overnight, a precipitate was obtained. It was collected, washed several times with diethyl ether, and then dried under vacuum to give **3b** as a yellow solid (169.4 mg, 0.156 mmol, 78%). ^{1}H NMR (400 MHz, DMSO-d_6, ppm): δ 10.73 (s, 1H, Ha), 8.33 (d, J = 8.0 Hz，2H, H6), 7.58 (m, 8H, H1/H2/H3/H5), 7.09 (d, J = 8.0 Hz, 2H, H4). ^{13}C NMR (100 MHz, DMSO-d_6, ppm): δ 155.5 (CO), 150.5 (C), 146.3 (C), 144.8 (C), 138.6 (C), 132.8 (C), 132.2 (C), 125.3 (CH), 124.1 (CH), 123.0 (CH), 118.6 (CH), 117.4 (CH), 117.1 (CH), 89.2 (C≡), 88.7 (C≡). ESI-MS: *m/z* 1086.26, $[M+H]^+$.

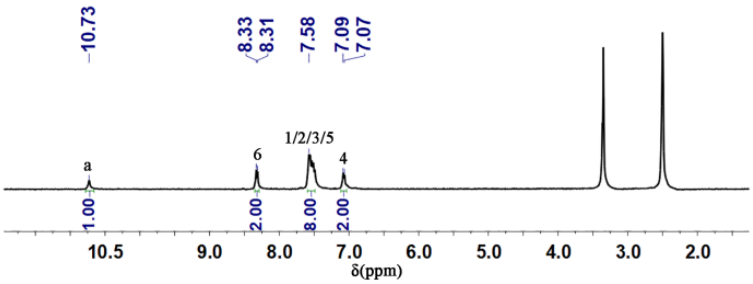

Fig. S12. ^{1}H NMR spectrum of **3b** (400 MHz, DMSO-d_6, 300 K).

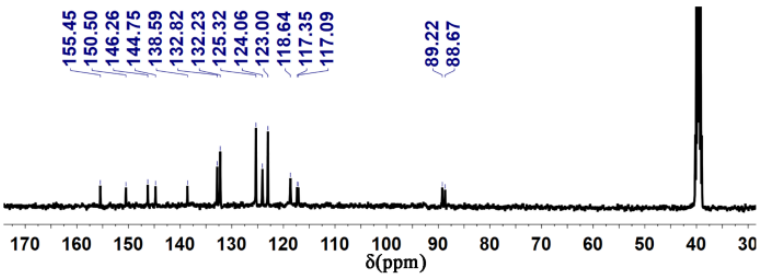

Fig. S13. ^{13}C NMR spectrum of **3b** (100 MHz, DMSO-d_6, 300 K).

Compound 3c:

To a THF solution (125 mL) of 4-nitrophenyl isocyanate (0.80 g, 4.80 mmol) was added a THF solution (20 mL) of 4-phenylenediamine (0.63 g, 5.8 mmol). Stirring 4 h at 0 ℃ afforded a precipitate, which was washed several times with diethyl ether and then dried in vacuum to yield **3c** as a yellow solid (1.14 g, 4.2 mmol, 87%). ^{1}H NMR (400 MHz, DMSO-d_6, ppm): δ 9.52 (s, 1H, Hc), 8.17 (d, J = 9.2 Hz, 2H, H6), 7.92 (s, 1H, Hb), 7.67 (d, J = 9.2 Hz, 2H, H5), 7.30 (d, J = 8.0 Hz, 1H, H4), 6.88 (t, J = 8.0 Hz, 1H, H3), 6.74 (d, J = 8.0 Hz, 1H, H1), 6.59 (t, J = 8.0 Hz, 1H, H2), 4.84 (s, 1H, Ha). ^{13}C NMR (100 MHz, DMSO-d_6, ppm): δ 153.1 (CO), 147.3 (C), 141.9 (C), 141.2 (C), 125.8 (C), 125.6 (CH), 124.9 (CH), 124.3 (CH), 117.7(CH), 117.24 (CH), 116.45 (CH), ESI-MS: m/z 273.09, $[M+H]^+$.

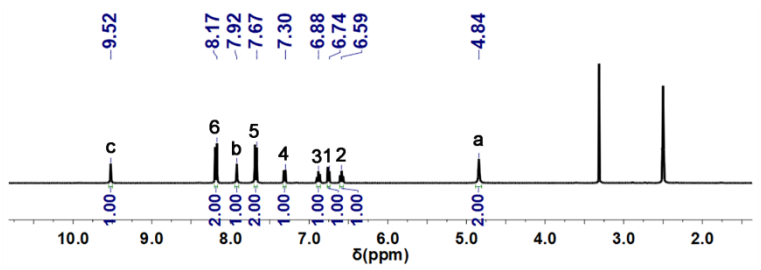

Fig. S14. ^{1}H NMR spectrum of **3c** (400 MHz, DMSO-d_6, 300 K).

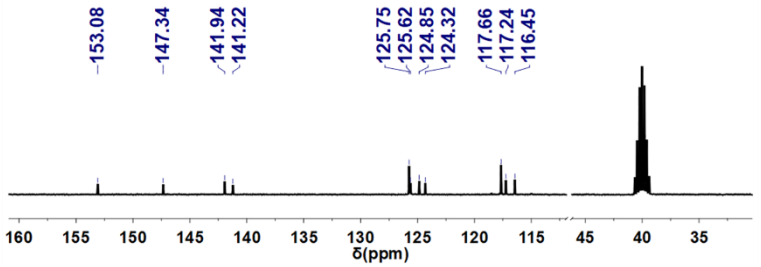

Fig. S15. ^{13}C NMR spectrum of **3c** (100 MHz, DMSO-d_6, 300 K).

Ligand L^3:

Compound **3b** (108 mg, 0.1 mmol) was dissolved in THF (10 mL) and added dropwise in a mixture of **3c** (113.6 mg) and Et_3N (0.1 mL) in THF (5 mL) and DMF (1 mL). Stirring overnight at room temperature afforded a precipitate, which was collected and washed several times with toluene, ethanol and diethyl ether, and then dried under vacuum to give $\mathbf{L^3}$ as a yellow solid (110 mg, 74%). ^{1}H NMR (400 MHz, DMSO-d_6, ppm): δ 9.85 (s, 1H, NHa), 9.31 (s, 1H, NHb), 8.29 (s, 1H, NHc), 8.19 (d, J = 9.2 Hz, 2H, H10), 8.16 (s, 1H, NHd), 7.73 (d, J = 9.2 Hz, 2H, H9), 7.62 (m, 2H, H5/8), 7.53 (d, J = 8.8 Hz, 1H, H4), 7.48 (d, J = 8.8 Hz, 2H, H2), 7.45 (d, J = 8.8 Hz, 2H, H3), 7.15 (t, 2H, H6/7), 7.09 (d, J = 8.8 Hz, 2H, H1). ^{13}C NMR (100 MHz, DMSO-d_6, ppm): δ 153.0 (CO), 152.7 (CO), 146.5 (C), 146.1 (C), 141.0 (C), 138.9 (C), 140.2 (C), 132.7 (C), 132.1 (C), 131.7 (C), 130.6 (CH), 125.1 (CH), 124.7 (CH), 124.6 (CH), 124.2 (CH), 124.1 (CH), 123.9 (CH), 118.4 (CH), 117.4 (CH), 115.3 (CH), 89.5 (C≡), 88.1 (C≡). ESI-MS: *m/z* 1485.47, $[M+H]^+$.

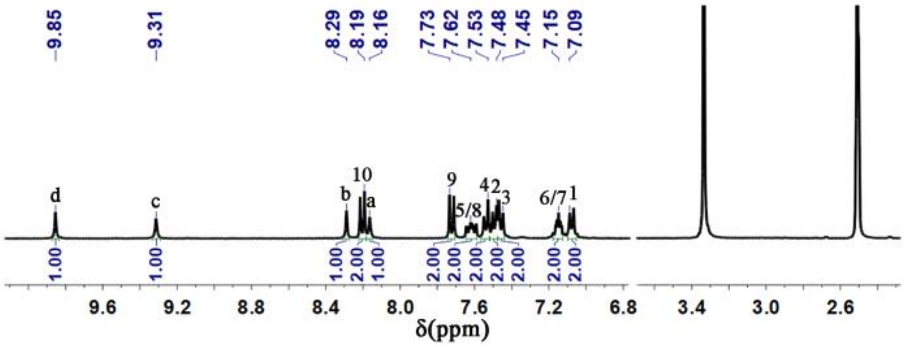

Fig. S16. ^{1}H NMR spectrum of $\mathbf{L^3}$ (400 MHz, DMSO-d_6, 300 K).

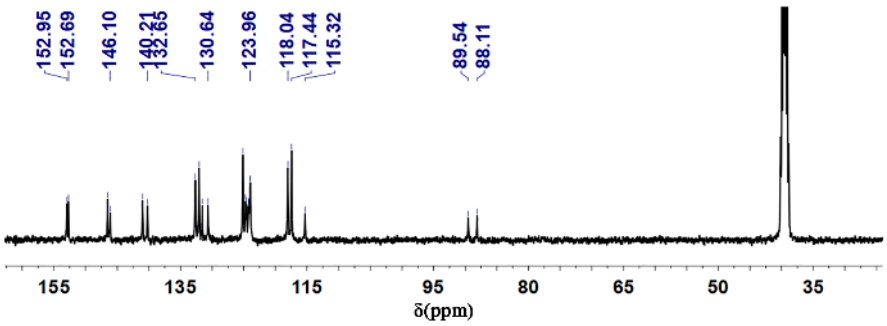

Fig. S17. ^{13}C NMR spectrum of $\mathbf{L^3}$ (100 MHz, DMSO-d_6, 300 K).

S3. Synthesis of anion complexes

S3.1 $(TBA)_6[(SO_4)_3(L^1)_2]$

Compound $(TBA)_6[(\mathbf{L^1})_2(SO_4)_3]$ was prepared according to reported procedures.[1] ^{1}H NMR (400 MHz, DMSO-d_6, ppm): δ 10.62 (s, 1H, NHd), 9.67 (s, 1H, NHc), 9.53 (s, 1H, NHb), 9.39 (s, 1H, Ha), 7.84 (m, 2H, H3/6), 7.78 (d, J = 8.4 Hz, H8), 7.55 (d, J = 8.4 Hz, 1H, H7), 7.40 (d, J = 8.4 Hz, 2H, H2), 7.02 (m, 2H, H4/5), 6.63 (d, J = 8.4 Hz, 2H, H1), 3.06 (t, 8H), 1.61 (m, 8H), 1.32 (m, 8H) and 0.88 (t, 12H) (TBA^+). ^{13}C NMR (150 MHz, DMSO-d_6, ppm): δ 153.1 (CO), 152.4 (CO), 147.1 (C), 141.9 (C), 140.7 (C), 153.0 (C), 130.5 (C), 129.8 (C), 124.9 (CH), 123.7 (CH), 123.5 (CH), 123.1 (CH), 119.8 (CH), 117.3 (CH), 57.5, 23.1, 19.2 and 13.5 (TBA^+).

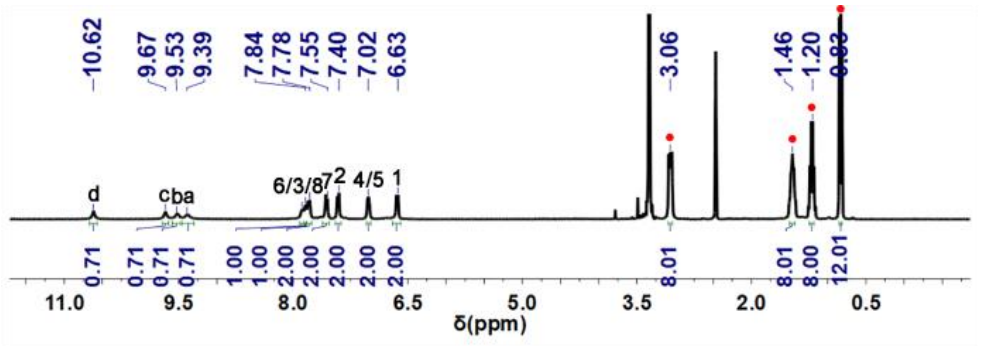

Fig. S18. ^{1}H NMR spectrum of complex $(TBA)_6[(SO_4)_3(\mathbf{L^1})_2]$ (400 MHz, DMSO-d_6, 300 K). • indicates signals of TBA.

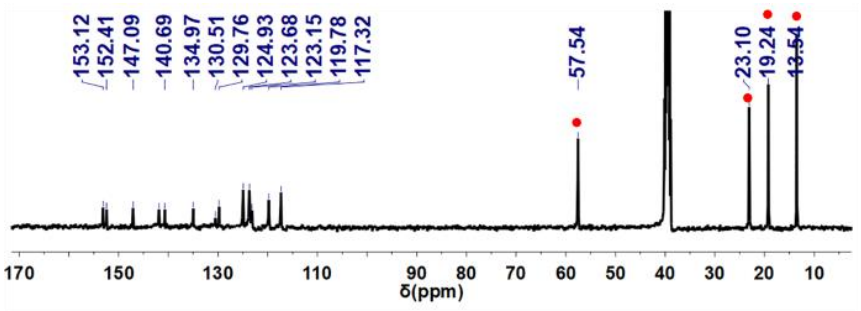

Fig. S19. ^{13}C NMR spectrum of complex $(TBA)_6[(SO_4)_3(\mathbf{L^1})_2]$ (150 MHz, DMSO-d_6, 300 K). • indicates signals of TBA.

S3.2 $(TBA)_{12}[(PO_4)_4(\mathbf{L^1})_4]$

Compound $(TBA)_{12}[(PO_4)_4(\mathbf{L^1})_4]$ was prepared according to reported procedures.[1] ^{1}H NMR (400 MHz, DMSO-d_6, ppm): δ 12.52 (s, 1H, NHd), 11.88 (s, 1H, NHc), 11.74 (s, 1H, NHb), 11.64 (s, 1H, Ha), 8.25 (d, J = 8.0 Hz, 1H, H6), 7.66 (m, 3H, H2/3), 7.56 (d, J = 8.4 Hz, 2H, H8), 7.36 (d, J = 8.4 Hz, 2H, H7), 6.96 (m, 1H, H4), 6.85 (m, 2H, H5), 6.35 (s, br, 2H, H1), 3.03 (t, 8H), 1.45 (m, 8H), 1.20 (m, 8H) and 0.83 (t, 12H) (TBA^+). ^{13}C NMR (150 MHz, DMSO-d_6, ppm): δ 153.8 (CO), 153.2 (CO), 148.2 (C), 141.1 (C), 139.5 (C), 135.3 (C), 132.8 (C), 128.6 (C), 124.0 (CH), 122.8 (CH), 120.5 (CH), 119.0 (CH), 117.6 (CH), 57.5, 23.0, 19.2 and 13.5 (TBA^+).

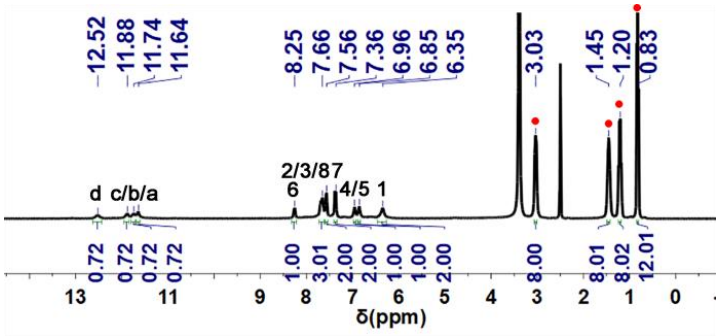

Fig. S20. ^{1}H NMR spectrum of complex $(TBA)_{12}[(PO_4)_4(\mathbf{L^1})_4]$ (400 MHz, DMSO-d_6, 300 K). • indicates signals of TBA.

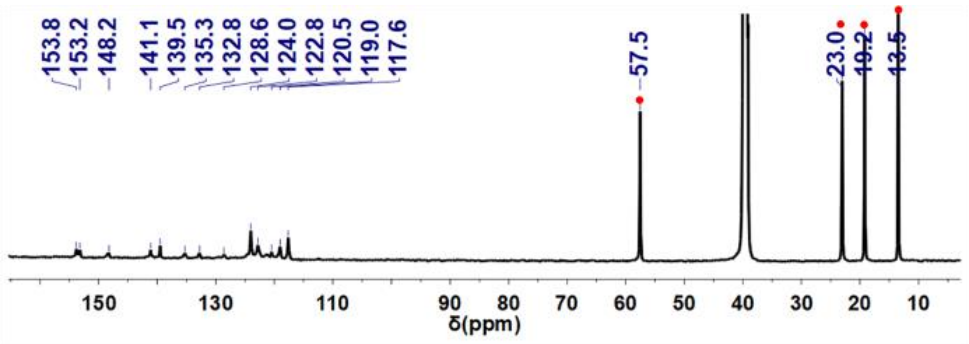

Fig. S21. ^{13}C NMR spectrum of complex $(TBA)_{12}[(PO_4)_4(\mathbf{L^1})_4]$ (150 MHz, DMSO-d_6, 300 K). • indicates signals of TBA.

S3.3 $(TBA)_{12}[(PO_4)_4(\mathbf{L^2})_4]$

$(TBA)_3PO_4$ (12 μL, 0.625 mol/L; generated in situ from H_3PO_4 and (TBA)OH in water) was added to a suspension of $\mathbf{L^2}$ (10 mg, 0.007 mmol) in acetonitrile (1 mL). After stirring 3 h at room temperature, a clear orange solution was obtained. Slow vapor diffusion of diethyl ether into this solution provided product $(TBA)_{12}[(PO_4)_4(\mathbf{L^2})_4]$ within two weeks (yield > 90%). ^{1}H NMR (400 MHz, DMSO-d_6, ppm): δ 12.68 (s, 1H, NHd), 12.11 (s, 1H, NHc), 11.94 (s, 1H, NHb), 11.68 (s, 1H, Ha), 8.20 (d, J = 7.2 Hz, 1H, H8), 7.87 (d, J = 8.0 Hz, 2H, H4), 7.82 (d, J = 7.2 Hz, 1H, H5), 7.61 (d, J = 8.4 Hz, 2H, H10), 7.42 (d, J = 8.4 Hz, 2H, H9), 7.12 (s, br, 2H, H2), 6.96 (m, 2H, H6/7), 6.69 (s, br, 2H, N3), 6.58 (s, br, 2H, H1), 3.05 (t, 8H), 1.47 (m, 8H), 1.24 (m, 8H) and 0.86 (t, 12H) (TBA^+). ^{13}C NMR (150 MHz, DMSO-d_6, ppm): δ 154.4 (CO), 153.6 (CO), 149.6 (C), 148.6 (C), 146.2 (C), 141.1 (C), 140.1 (C), 135.0 (C), 132.5 (C), 128.8 (C), 127.1 (CH), 126.5 (CH), 124.6 (CH), 124.0 (CH), 123.5 (CH), 121.7 (CH), 120.4 (CH), 118.0 (CH), 57.5, 23.0, 19.2 and 13.5 (TBA^+).

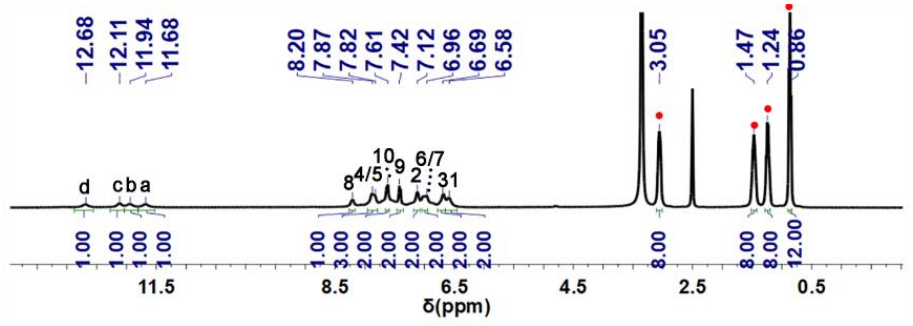

Fig. S22. ^{1}H NMR spectrum of complex $(TBA)_{12}[(PO_4)_4(\mathbf{L^2})_4]$ (400 MHz, DMSO-d_6, 300 K). • indicates signals of TBA.

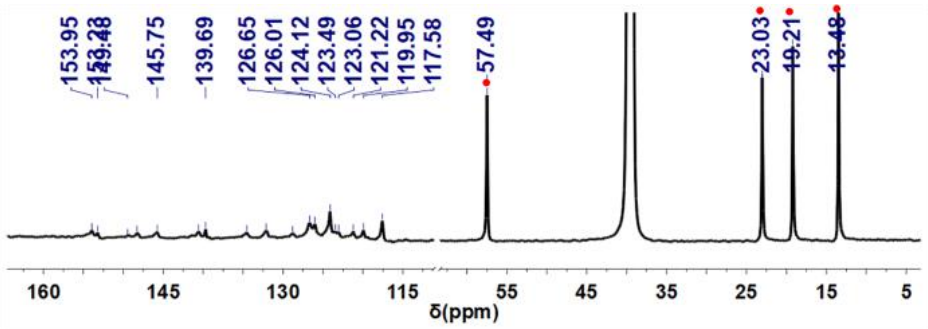

Fig. S23. ^{13}C NMR spectrum of complex $(TBA)_{12}[(PO_4)_4(\mathbf{L}^2)_4]$ (150 MHz, DMSO-d_6, 300 K). • indicates signals of TBA.

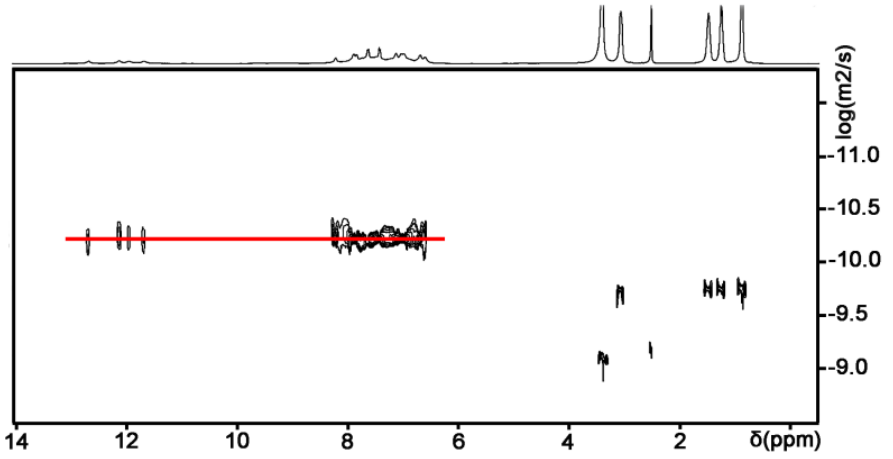

Fig. S24. DOSY spectrum of $(TBA)_{12}[(PO_4)_4(\mathbf{L}^2)_4]$ (400 MHz, DMSO-d_6, 300 K).

The hydrodynamic radius was estimated according to the Stokes-Einstein Equation, $D = kT/6\pi\eta r$, where D is the diffusion constant, k is the Boltzmann's constant, T is the temperature, η is the viscosity of solvents, and r is the radius. $D = 5.36*10^{-11}$ m^2s^{-1}, $k = 1.38*10^{-23}$ NmK^{-1}, $T = 300$ K, $\eta = 1.991*10^{-2}$ g $cm^{-1}s^{-1}$. $r = kT/6\pi\eta D = 20.6$ Å. The radius of the DFT-optimized $(TBA)_{12}[(PO_4)_4(\mathbf{L}^2)_4]$ structure was 20.5 Å.

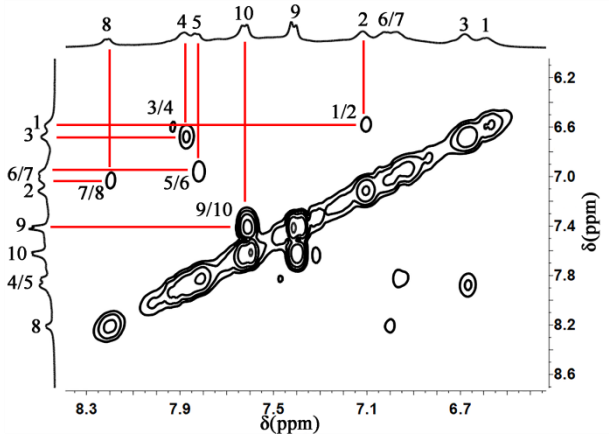

Fig. S25. ^{1}H-^{1}H COSY spectrum of $(TBA)_{12}[(PO_4)_4(\mathbf{L}^2)_4]$ (400 MHz, DMSO-d_6, 300 K).

S3.4 $(TBA)_6[(SO_4)_3(\mathbf{L}^2)_2]$

$(TBA)_2SO_4$ (17 µL, 0.625 mol/L;) was added to a suspension of $\mathbf{L}^2$ (10 mg, 0.007 mmol) in acetonitrile (1 mL). After stirring 3 h at room temperature, a clear orange solution was obtained. Slow vapor diffusion of diethyl ether into this solution provided product $(TBA)_6[(SO_4)_3(\mathbf{L}^2)_2]$ within two weeks (yield > 90 %). ^{1}H NMR (400 MHz, DMSO-d_6, ppm): δ 10.70 (s, 1H, Hd), 9.88 (s, 1H, Hc), 9.50 (s, 1H, Hb/a), 7.90 (m, 4H, H5/8/10), 7.65 (d, J = 8.0 Hz, 4H, H4/9), 7.49 (d, J = 8.0 Hz, 2H, H2), 7.40 (d, J = 8.0 Hz, 2H, H3), 7.08 (s, br, 2H, H6/7), 6.98 (d, J = 8.0 Hz, 2H, H3), 3.12 (t, 8H), 1.53 (m, 8H), 1.27 (m, 8H) and 0.90 (t, 12H) (TBA^+). ^{13}C NMR (150 MHz, DMSO-d_6, ppm): δ 153.0 (CO), 152.3 (CO), 147.1 (C), 145.6 (C), 140.6 (C), 139.5 (C), 134.1 (C), 132.5 (C), 130.0 (C), 129.7 (C), 127.0 (CH), 126.2 (CH), 124.9 (CH), 124.1 (CH), 123.6 (CH), 123.4 (CH), 123.1 (CH), 122.9 (CH), 119.1 (CH), 117.3 (CH), 57.6, 23.1, 19.2 and 13.6 (TBA^+).

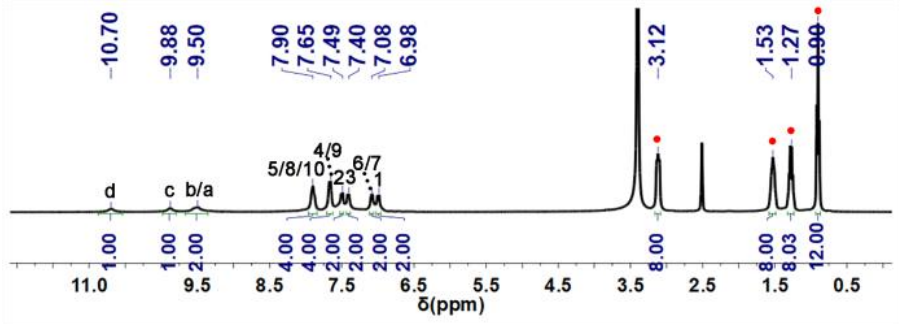

Fig. S26. ^{1}H spectrum of $(TBA)_6[(SO_4)_3(\mathbf{L}^2)_2]$(400 MHz, DMSO-$d_6$, 300 K). • indicates signals of TBA.

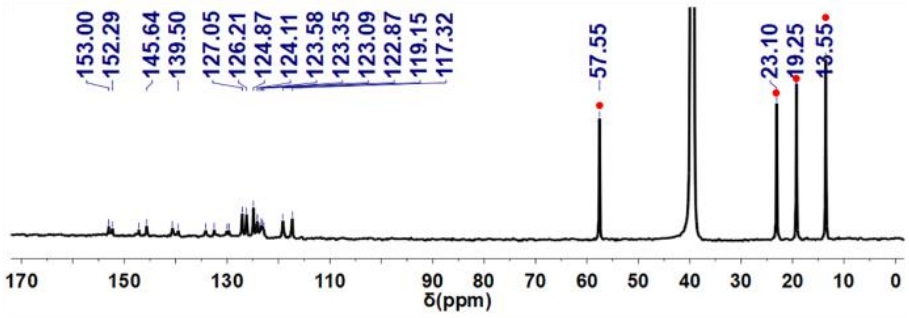

Fig. S27. ^{13}C NMR spectrum of complex $(TBA)_6[(SO_4)_3(\mathbf{L}^2)_2]$ (150 MHz, DMSO-d_6, 300 K). • indicates signals of TBA.

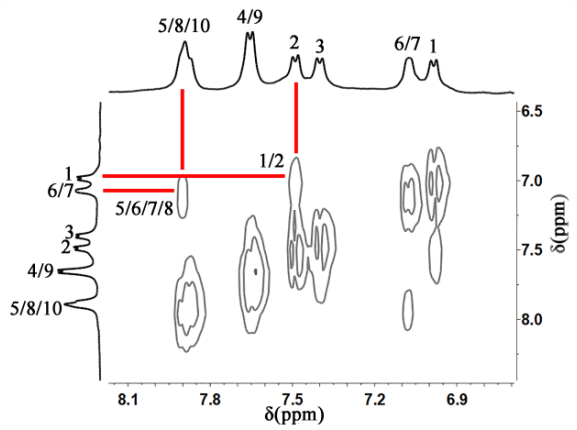

Fig. S28. COSY spectra of $(TBA)_6[(SO_4)_3(\mathbf{L}^2)_2]$ (400 MHz, DMSO-d_6, 300 K).

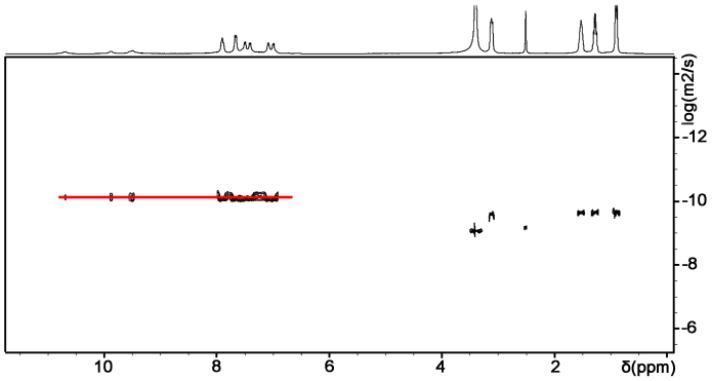

Fig. S29. DOSY spectrum of $(TBA)_6[(SO_4)_3(\mathbf{L}^2)_2]$ (400 MHz, DMSO-d_6, 300 K).

The sphere's hydrodynamic radius was estimated according to the Stokes-Einstein Equation, $D = kT/6\pi\eta r$, where D is the diffusion constant, k is the Boltzmann's constant, T is the temperature, η is the viscosity of solvents, and r is the radius. D = 6.72*10^{-11} m^{2}s^{-1}, k = 1.38*10^{-23} NmK^{-1}, T = 300 K, η = 1.991*10^{-2} g cm^{-1}s^{-1}. $r = kT/6\pi\eta D$ = 16.4 Å. The radius of the optimized $(TBA)_6[(SO_4)_3(\mathbf{L}^2)_2]$ structure was 19.4 Å.

S3.5 $(TBA)_{12}[(PO_4)_4(\mathbf{L}^3)_4]$

$(TBA)_3PO_4$ (11 µL, 0.625 mol/L; generated in situ from H_3PO_4 and (TBA)OH in water) was added to a suspension of $\mathbf{L}^3$ (10 mg, 0.007 mmol) in acetonitrile (1 mL). After stirring 3 h at room temperature, a clear yellow solution was obtained. Slow vapor diffusion of diethyl ether into this solution provided product of $(TBA)_{12}[(PO_4)_4(\mathbf{L}^2)_4]$ within two weeks (yield > 90 %).^{1}H NMR (400 MHz, DMSO-d_6, ppm): δ 12.89 (s, 1H, NHd), 12.04 (s, 2H, NHc/b), 11.61 (s, 1H, Ha), 8.19 (s, br, 1H, H8), 8.04 (s, br, 1H, H5), 7.75 (d, J = 8.0 Hz, 2H, H4), 7.63 (d, J = 8.0 Hz, 2H, H10), 7.44 (d, J = 8.0 Hz, 2H, H9), 7.30 (d, J = 8.0 Hz, 2H, H1), 6.96(m, 2H, H6/7), 6.83 (d, J = 8.0 Hz, 2H, H2), 6.80 (d, J = 8.0 Hz, 2H, H3), 3.08 (t, 8H), 1.50 (m, 8H), 1.26 (m, 8H) and 0.88 (t, 12H) (TBA^+). ^{13}C NMR (150 MHz, DMSO-d_6, ppm): δ 153.5 (CO), 153.2 (CO), 148.2 (C), 145.9 (C), 141.8 (C), 139.7 (C), 132.6 (C), 131.3 (C), 128.7 (C), 124.1 (C), 123.6 (CH), 123.1 (CH), 122.9 (CH), 121.3 (CH), 120.8 (CH), 118.5 (CH), 117.4 (CH), 113.8 (CH), 89.9 (C≡), 87.5 (C≡),57.5, 23.1, 19.2 and 13.5 (TBA^+).

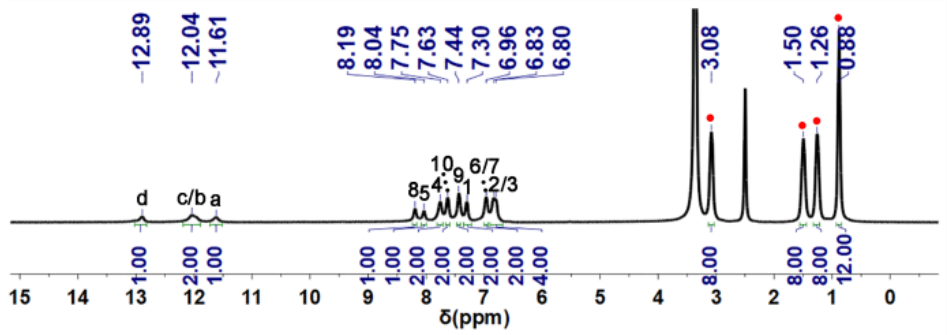

Fig. S30. ^{1}H spectrum of complex $(TBA)_{12}[(PO_4)_4(\mathbf{L^3})_4]$ (400 MHz, DMSO-d_6, 300 K). • indicates signals of TBA.

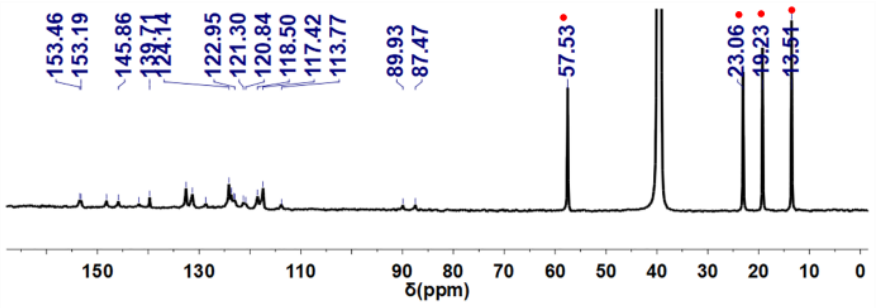

Fig. S31. ^{13}C spectrum of complex $(TBA)_{12}[(PO_4)_4(\mathbf{L^3})_4]$ (150 MHz, DMSO-d_6, 300 K). • indicates signals of TBA.

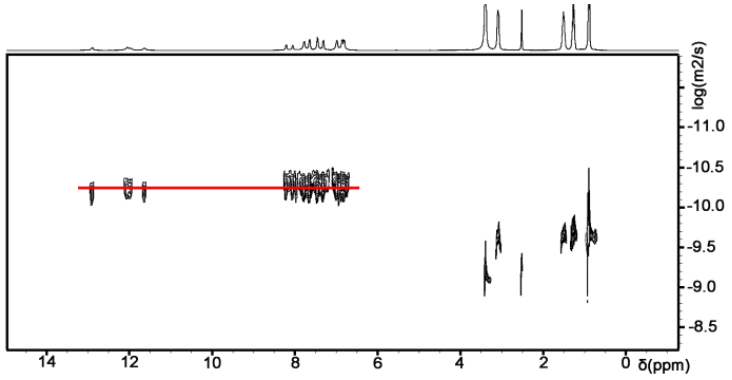

Fig. S32. DOSY spectrum of $(TBA)_{12}[(PO_4)_4(\mathbf{L^3})_4]$(400 MHz, DMSO-$d_6$, 300 K).

The sphere's hydrodynamic radius was estimated according to the Stokes-Einstein Equation, $D = kT/6\pi\eta r$, where D is the diffusion constant, k is the Boltzmann's constant, T is the temperature, η is the viscosity of solvents, and r is the radius. D = 4.30*10^{-11} m^{2}s^{-1}, k = 1.38*10^{-23} NmK^{-1}, T = 300 K, η = 1.991*10^{-2} g cm^{-1}s^{-1}. $r = kT/6\pi\eta D$ = 25.7 Å. The radius of the optimized $(TBA)_{12}[(PO_4)_4(\mathbf{L^3})_4]$ structure was 23.8 Å.

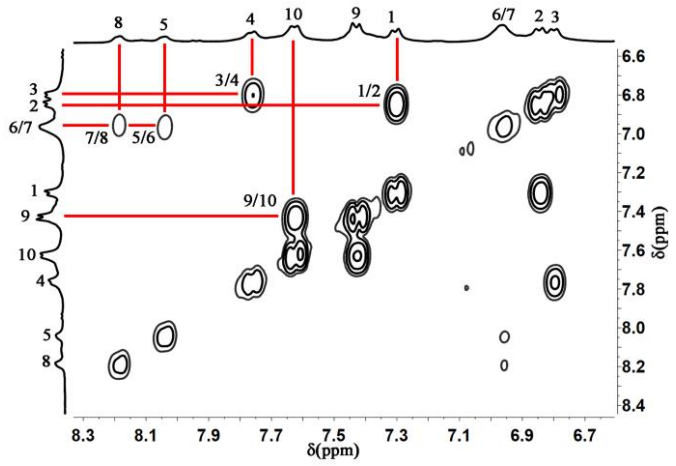

Fig. S33. ^{1}H-^{1}H COSY spectrum of $(TBA)_{12}[(PO_4)_4(\mathbf{L}^3)_4]$ (400 MHz, DMSO-d_6, 300 K).

S3.6 $(TBA)_6[(SO_4)_3(\mathbf{L}^3)_2]$

$(TBA)_2SO_4$ (16 µL, 0.625 mol/L;) was added to a suspension of $\mathbf{L}^3$ (10 mg, 0.007 mmol) in acetonitrile (1 mL). After stirring 3 h at room temperature, a clear yellow solution was obtained. Slow vapor diffusion of diethyl ether into this solution provided product $(TBA)_6[(SO_4)_3(L^3)_2]$ within two weeks (yield > 90 %). ^{1}H NMR (400 MHz, DMSO-d_6, ppm): δ 10.56 (s, 1H, NHd), 9.94 (s, 1H, NHc), 9.38 (s, 1H, Hb/a), 7.87 (m, 4H, H5/8/10), 7.62 (d, J=8.0 Hz, 4H, H4/9), 7.41 (d, J=8.0 Hz, 2H, H1), 7.27 (d, J=8.0 Hz, 2H, H2), 7.07 (s, br, 2H, H6/7), 6.88 (d, J=8.0 Hz, 2H, H3), 3.11 (t, 8H), 1.52 (m, 8H), 1.27 (m, 8H) and 0.90 (t, 12H) (TBA^+). ^{13}C NMR (150 MHz, DMSO-d_6, ppm): δ 152.8 (CO), 152.3 (CO), 147.1 (C), 145.7 (C), 140.8 (C), 140.7 (C), 132.8 (C), 131.9 (C), 129.8 (C), 124.9 (C), 123.8 (CH), 123.6 (CH), 123.4 (CH), 122.8 (CH), 118.5 (CH), 117.6 (CH), 117.3 (CH), 115.1 (CH), 89.7 (C≡), 88.0 (C≡), 57.6, 23.1, 19.3 and 13.6 (TBA^+).

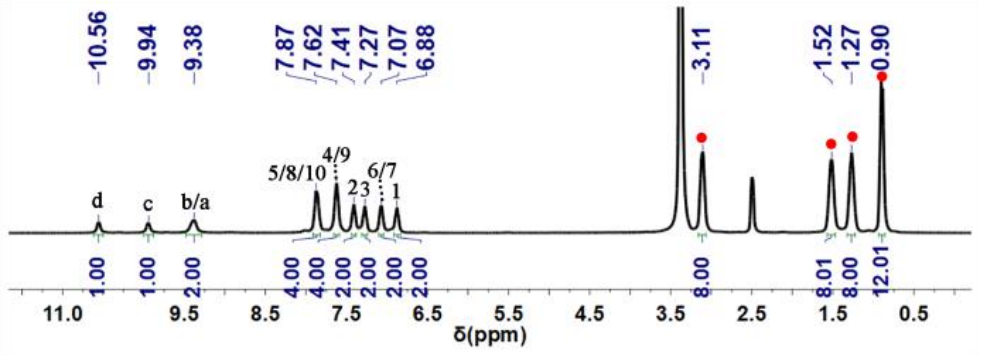

Fig. S34. ^{1}H spectrum of $(TBA)_6[(SO_4)_3(\mathbf{L}^3)_2]$ (400 MHz, DMSO-d_6, 300 K). • indicates signals of TBA.

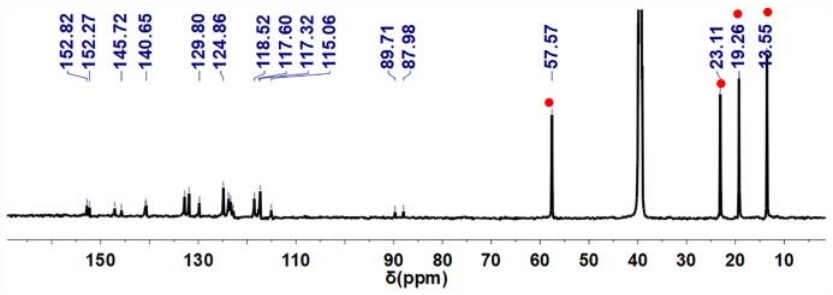

Fig. S35. ^{13}C NMR spectrum of complex (TBA)$_6$[(SO$_4$)$_3$(**L**^{3})$_2$] (150 MHz, DMSO-d_6, 300 K). • indicates signals of TBA.

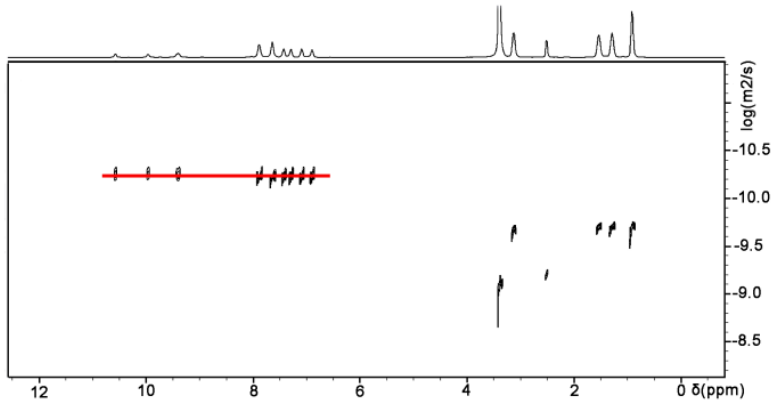

Fig. S36. DOSY spectra of (TBA)$_6$[(SO$_4$)$_3$(**L**^{3})$_2$] (400 MHz, DMSO-d_6, 300 K).

The sphere's hydrodynamic radius was estimated according to the Stokes-Einstein Equation, $D = kT/6\pi\eta r$, where D is the diffusion constant, k is the Boltzmann's constant, T is the temperature, η is the viscosity of solvents, and r is the radius. D = 5.47*10^{-11} m^{2}s^{-1}, k = 1.38*10^{-23} NmK^{-1}, T = 300 K, η = 1.991*10^{-2} g cm^{-1}s^{-1}. $R = kT/6\pi\eta D$ = 20.2 Å. The radius of the optimized (TBA)$_6$[(**L**^{3})$_2$(SO$_4$)$_3$] structure was 22.7 Å.

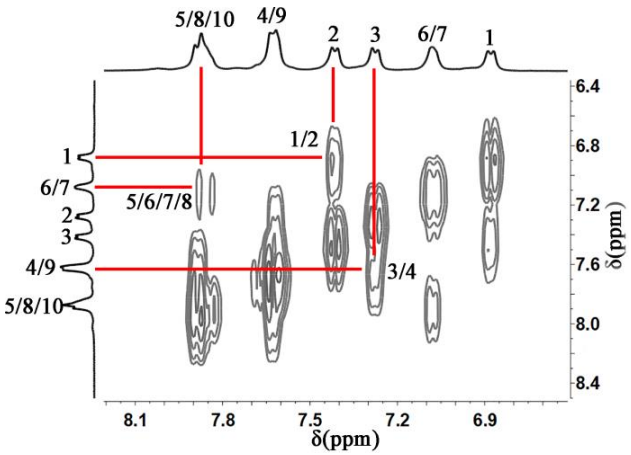

Fig. S37. COSY spectra of (TBA)$_6$[(SO$_4$)$_3$(**L**^{3})$_2$] (400 MHz, DMSO-d_6, 300 K).

S3.7 Synthesis of $(TBA)_6[(SO_4)_3(L^1)_2]$, $(TBA)_6[(SO_4)_3(L^2)_2]$ and $(TBA)_6[(SO_4)_3(L^3)_2]$ by self-sorting.

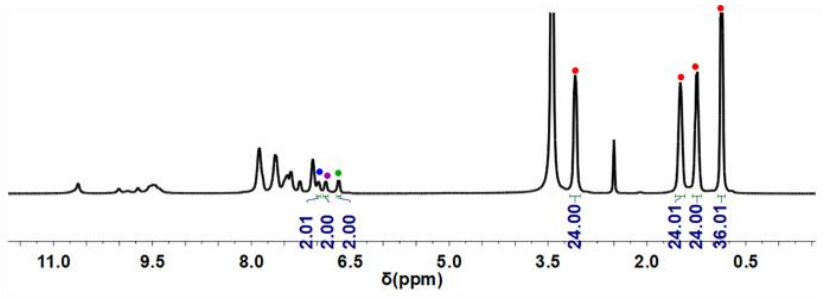

Fig. S38. ^{1}H NMR spectrum of self-sorted $(TBA)_6[(SO_4)_3(\mathbf{L}^1)_2]$, $(TBA)_6[(SO_4)_3(\mathbf{L}^2)_2]$ and $(TBA)_6[(SO_4)_3(\mathbf{L}^3)_2]$ (400 MHz, DMSO-d_6, 300 K). • (red) indicates signals of TBA, • (light green) indicates signals of $(TBA)_6[(SO_4)_3(\mathbf{L}^1)_2]$, • (blue) indicates signals of $(TBA)_6[(SO_4)_3(\mathbf{L}^2)_2]$, • (purple) indicates signals of $(TBA)_6[(SO_4)_3(\mathbf{L}^3)_2]$.

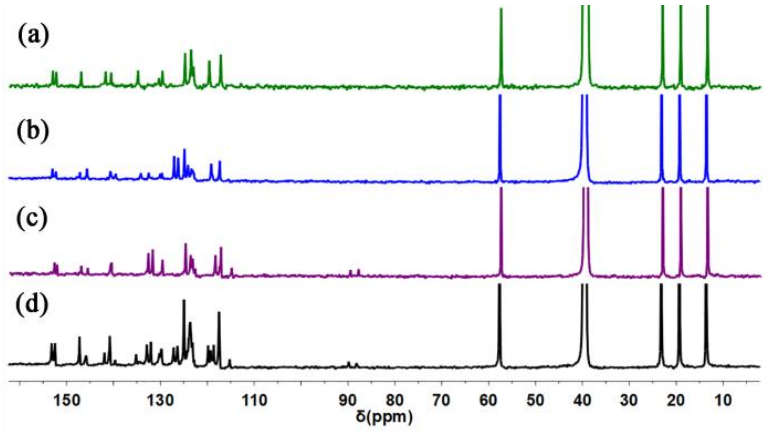

Fig. S39. ^{13}C NMR spectra of sulfate complexes $(TBA)_6[(SO_4)_3(\mathbf{L})_2]$: a) with $\mathbf{L}^3$; b) with $\mathbf{L}^2$; c) with $\mathbf{L}^1$; d) complex mixture from ligands $\mathbf{L}^1$, $\mathbf{L}^2$ and $\mathbf{L}^3$ (150 MHz, 300 K, DMSO-d_6).

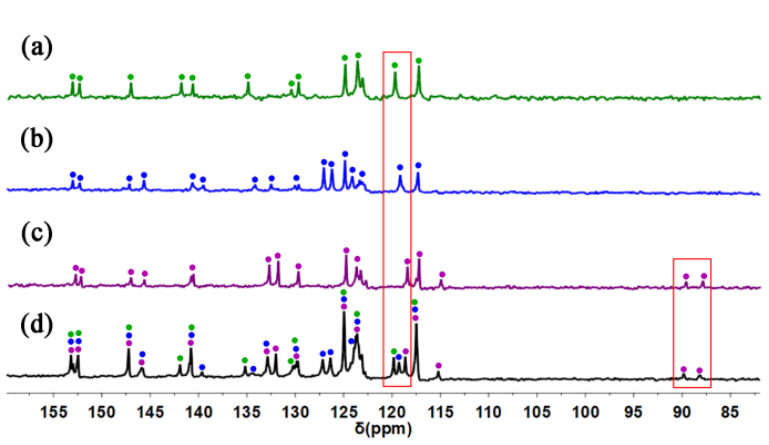

Fig. S40. Section of the ^{13}C NMR spectra of sulfate complexes $(TBA)_6[(SO_4)_3(\mathbf{L})_2]$: a) with $\mathbf{L}^3$; b) with $\mathbf{L}^2$; c) with $\mathbf{L}^1$; d) complex mixture from ligands $\mathbf{L}^1$, $\mathbf{L}^2$ and $\mathbf{L}^3$ (150 MHz, 300 K, DMSO-d_6).

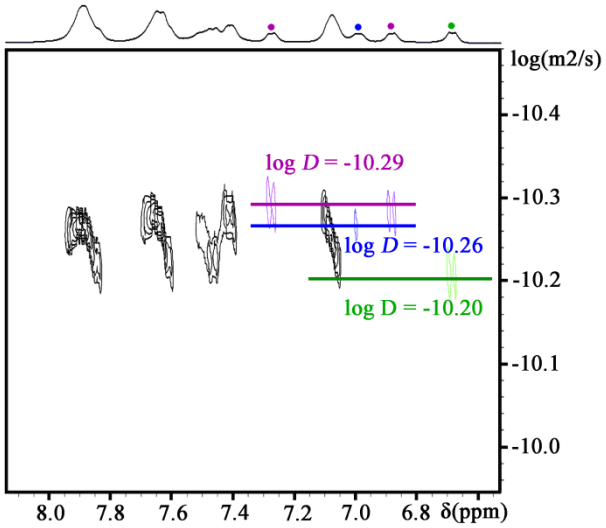

Fig. S41. DOSY spectra of self-sorted $(TBA)_6[(SO_4)_3(\mathbf{L^1})_2]$, $(TBA)_6[(SO_4)_3(\mathbf{L^2})_2]$ and $(TBA)_6[(SO_4)_3(\mathbf{L^3})_2]$ (400 MHz, DMSO-d_6, 300 K). Diffusion coefficient for $(TBA)_6[(SO_4)_3(\mathbf{L^3})_2]$, $D = 5.128 \times 10^{-11}$ m^2s^{-1}, log $D = -10.29$, $r = 21.5$ Å, for $(TBA)_6[(SO_4)_3(\mathbf{L^2})_2]$ $D = 5.495 \times 10^{-11}$ m^2s^{-1} , log $D = -10.26$, $r = 20.0$ Å, for $(TBA)_6[(SO_4)_3(\mathbf{L^1})_2]$ $D = 6.310 \times 10^{-11}$ m^2s^{-1} , log $D = -10.20$, $r = 17.5$ Å. • (light green) indicates signals of $(TBA)_6[(SO_4)_3(\mathbf{L^1})_2]$, • (blue) indicates signals of $(TBA)_6[(SO_4)_3(\mathbf{L^2})_2]$, • (purple) indicates signals of $(TBA)_6[(SO_4)_3(\mathbf{L^3})_2]$.

S3.8 Synthesis of $(TBA)_{12}[(PO_4)_4(\mathbf{L^1})_4]$, $(TBA)_{12}[(PO_4)_4(\mathbf{L^2})_4]$ and $(TBA)_{12}[(PO_4)_4(\mathbf{L^3})_3]$ by self-sorting.

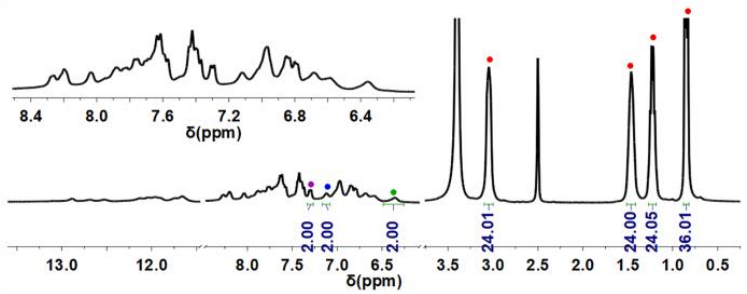

Fig. S42. ^{1}H spectrum of self-sorted complex mixture $(TBA)_{12}[(PO_4)_4(\mathbf{L^1})_4]$, $(TBA)_{12}[(PO_4)_4(\mathbf{L^2})_4]$ and $(TBA)_{12}[(PO_4)_4(\mathbf{L^3})_4]$ (400 MHz, DMSO-d_6, 300 K). • (red) indicates signals of TBA, • (light green) indicates signals of $(TBA)_{12}[(PO_4)_4(\mathbf{L^1})_4]$, • (blue) indicates signals of $(TBA)_{12}[(PO_4)_4(\mathbf{L^2})_4]$, • (purple) indicates signals of $(TBA)_{12}[(PO_4)_4(\mathbf{L^3})_4]$.

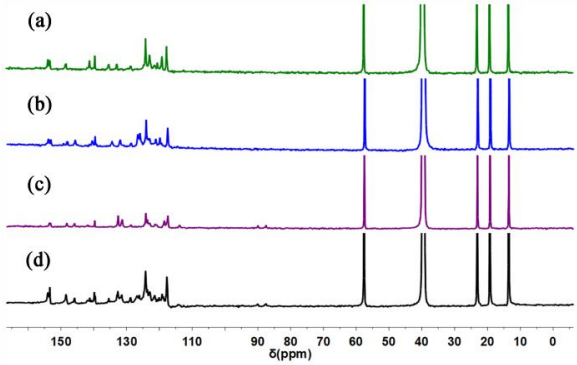

Fig. S43. ^{13}C NMR spectra of phosphate complexes $(TBA)_{12}[(PO_4)_4(\mathbf{L})_4]$: a) with $\mathbf{L^1}$; b) with $\mathbf{L^2}$; c) with $\mathbf{L^3}$; d) complex mixture from ligands $\mathbf{L^1}$, $\mathbf{L^2}$ and $\mathbf{L^3}$ (150 MHz, 300 K, DMSO-d_6).

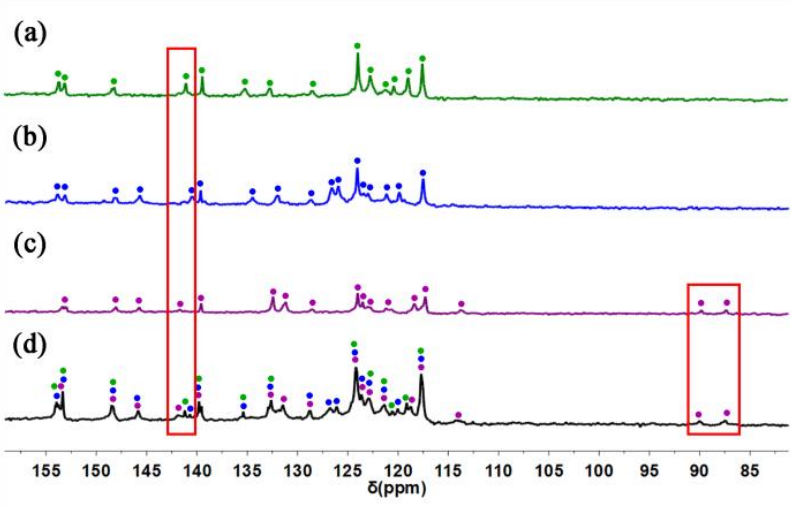

Fig. S44. Section of the ^{13}C NMR spectra of phosphate complexes $(TBA)_{12}[(PO_4)_4(\mathbf{L})_4]$: a) with $\mathbf{L}^1$; b) with $\mathbf{L}^2$; c) with $\mathbf{L}^3$; d) complex mixture from ligands $\mathbf{L}^1$, $\mathbf{L}^2$ and $\mathbf{L}^3$ (150 MHz, 300 K, DMSO-d_6).

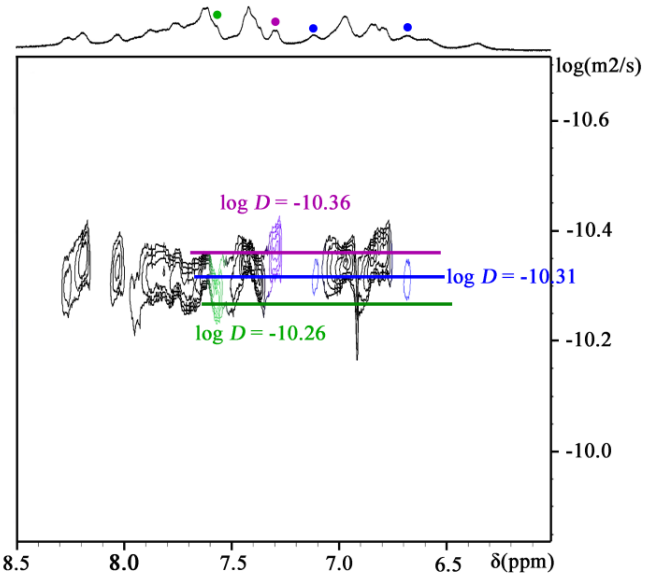

Fig. S45. DOSY spectra of self-sorted complex mixture $(TBA)_{12}[(PO_4)_4(\mathbf{L}^1)_4]$, $(TBA)_{12}[(PO_4)_4(\mathbf{L}^2)_4]$ and $(TBA)_{12}[(PO_4)_4(\mathbf{L}^3)_4]$ (400 MHz, DMSO-d_6, 300 K). Diffusion coefficient for $(TBA)_{12}[(PO_4)_4(\mathbf{L}^3)_4]$, D = 4.365×10^{-11} m^2s^{-1}, log D = −10.36, r = 25.3 Å, for $(TBA)_{12}[(PO_4)_4(\mathbf{L}^2)_4]$ D = 4.898×10^{-11} m^2s^{-1} , log D = −10.31, r = 22.5 Å, for $(TBA)_{12}[(PO_4)_4(\mathbf{L}^1)_4]$ D = 5.495×10^{-11} m^2s^{-1} , log D = −10.26, r = 20.0 Å. • (light green) indicates signals of $(TBA)_{12}[(PO_4)_4(\mathbf{L}^1)_4]$, • (blue) indicates signals of $(TBA)_{12}[(PO_4)_4(\mathbf{L}^2)_4]$, • (purple) indicates signals of $(TBA)_{12}[(PO_4)_4(\mathbf{L}^3)_4]$.

S4. HR ESI-MS studies.

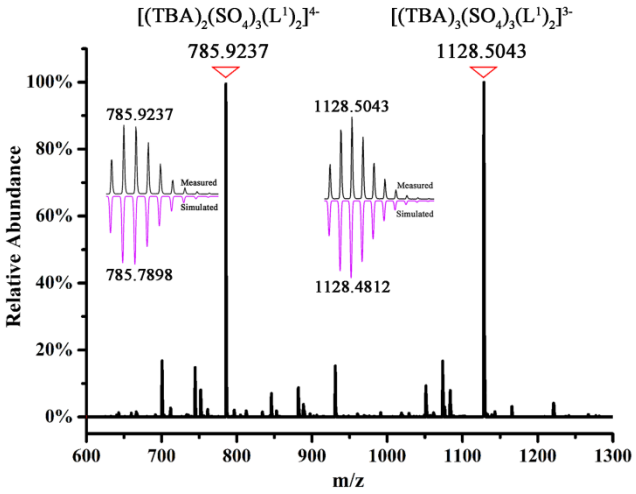

Fig. S46. HR ESI-MS spectrum of $(TBA)_6[(SO_4)_3(\mathbf{L^1})_2]$ with measured and simulated peaks (negative ions).

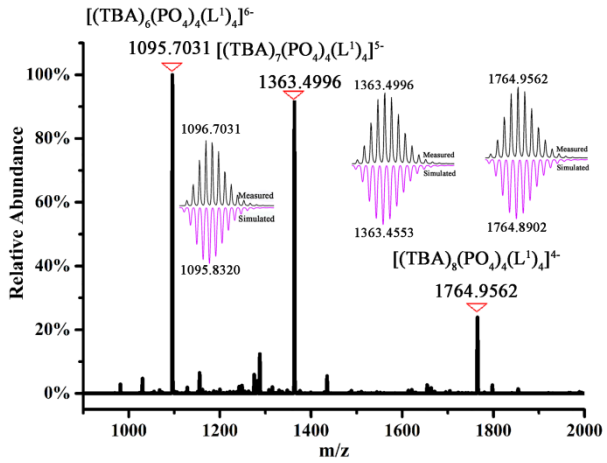

Fig. S47. HR ESI-MS spectrum of $(TBA)_{12}[(PO_4)_4(\mathbf{L^1})_4]$ with measured and simulated peaks (negative ions).

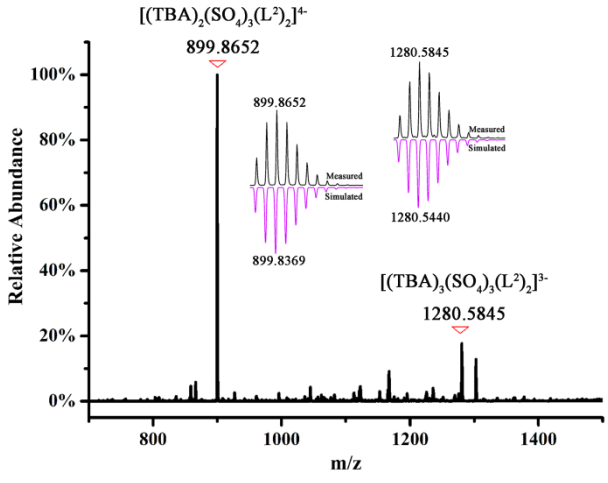

Fig. S48. HR ESI-MS spectrum of $(TBA)_6[(SO_4)_3(\mathbf{L^2})_2]$. Measured and simulated peaks (negative ions).

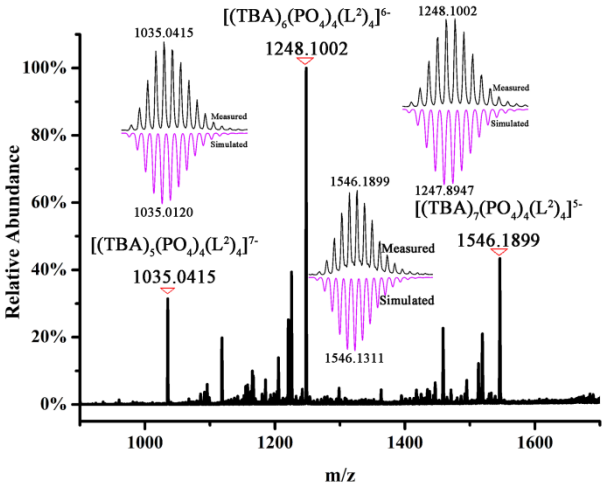

Fig. S49. HR ESI-MS spectrum of $(TBA)_{12}[(PO_4)_4(\mathbf{L}^2)_4]$. Measured and simulated peaks (negative ions).

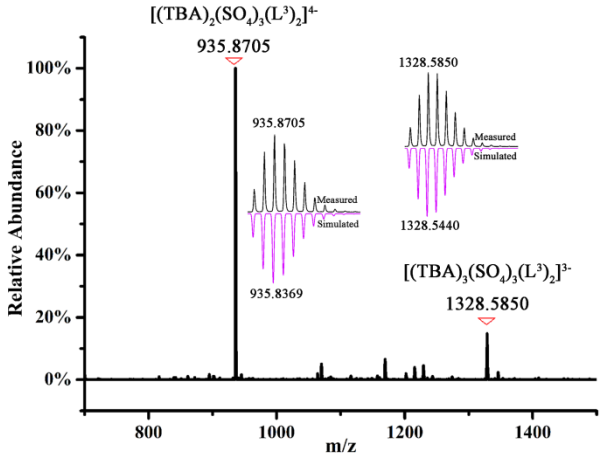

Fig. S50. HR ESI-MS spectrum of $(TBA)_6[(SO_4)_3(\mathbf{L}^3)_2]$. Measured and simulated peaks (negative ions).

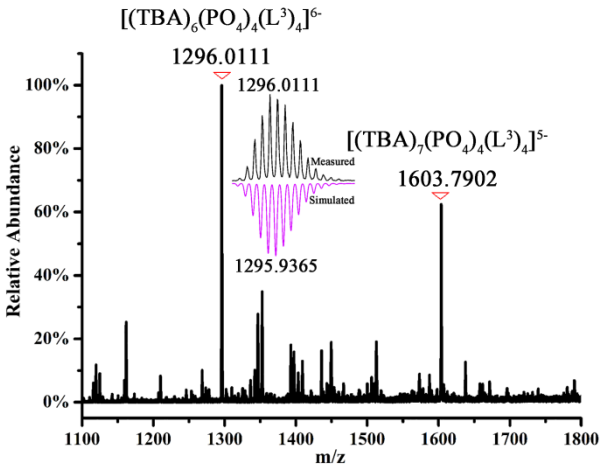

Fig. S51. HR ESI-MS spectrum of $(TBA)_{12}[(PO_4)_4(\mathbf{L}^3)_4]$. Measured and simulated peaks (negative ions).

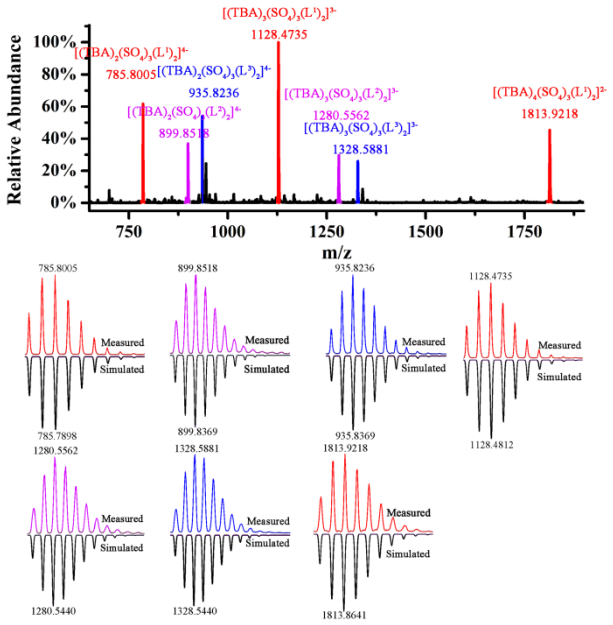

Fig. S52. HR ESI-MS spectrum of the complex mixture of $(TBA)_6[(SO_4)_3(\mathbf{L^1})_2]$, $(TBA)_6[(SO_4)_3(\mathbf{L^2})_2]$ and $(TBA)_6[(SO_4)_3(\mathbf{L^3})_2]$ with measured and simulated peaks (negative ions).

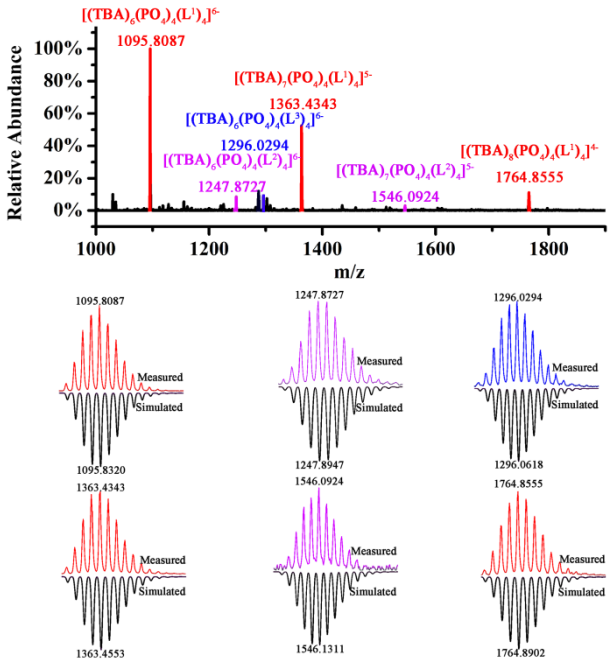

Fig. S53. HR ESI-MS spectrum of the complex mixture of $(TBA)_{12}[(PO_4)_4(\mathbf{L^1})_4]$, $(TBA)_{12}[(PO_4)_4(\mathbf{L^2})_4]$ and $(TBA)_{12}[(PO_4)_4(\mathbf{L^3})_4]$ with measured and simulated peaks (negative ions).

S5. Simulated molecular model of complexes.

The geometries of the sulfate complexes were optimized at B97-3c level[2] of theory as implemented in the ORCA package (version 4.1.0)[3] while the phosphate complexes at semiempirical density functional tight binding (DFTB) GFN-xTB[4] level using a stand-alone program xtb (version 6.1) from Prof. Grimme's group.[5] The initial geometry was built manually from the crystal structures of $[(SO_4)_3(\mathbf{L^1})_2]^{6-}$ and

$[(PO_4)_4(\mathbf{L^1})_4]^{12-}$.

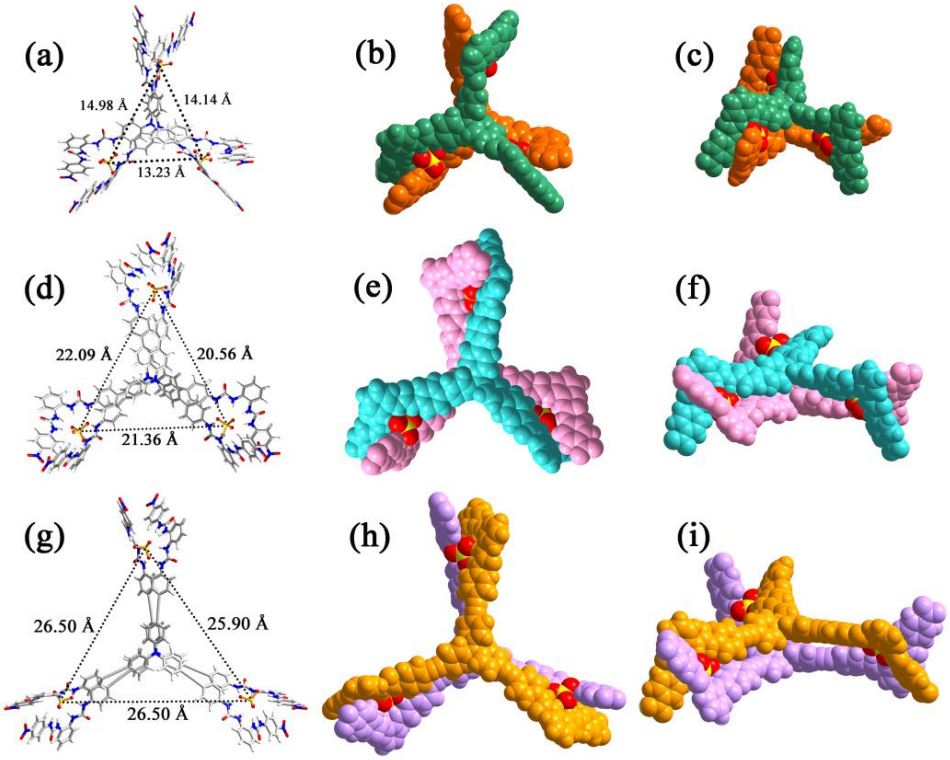

Fig. S54. Optimized structures of the "pinwheel" helical sulfate complexes: (a) $[(SO_4)_3(\mathbf{L^1})_2]^{6-}$; (b, c) top and side view of the space-filling representation of $[(SO_4)_3(\mathbf{L^1})_2]^{6-}$. (d) $[(SO_4)_3(\mathbf{L^2})_2]^{6-}$; (e, f) top and side view of the space-filling representation of $[(SO_4)_3(\mathbf{L^2})_2]^{6-}$. (g) $[(SO_4)_3(\mathbf{L^3})_2]^{6-}$; (h, i) top and side view of the space-filling representation of $[(SO_4)_3(\mathbf{L^3})_2]^{6-}$. Only a ΔΔΔ enantiomer is shown.

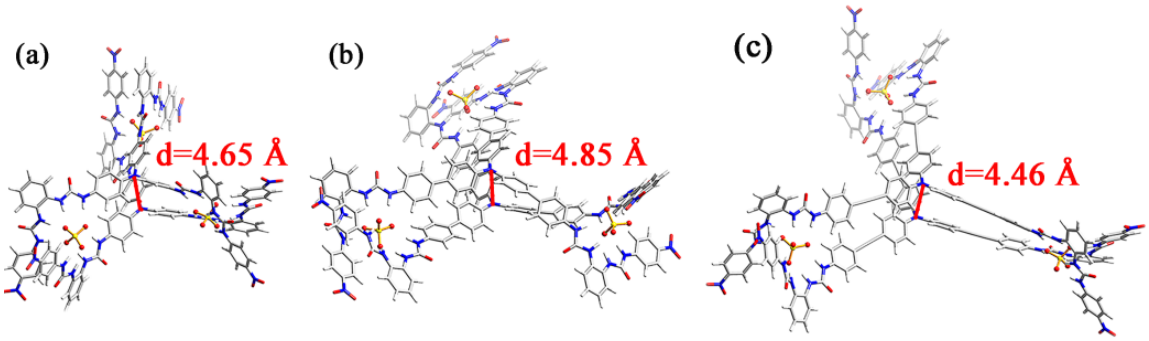

Fig. S55. The distance between ligands (a) $[(SO_4)_3(\mathbf{L^1})_2]^{6-}$; (b) $[(SO_4)_3(\mathbf{L^2})_2]^{6-}$; (c) $[(SO_4)_3(\mathbf{L^3})_2]^{6-}$.

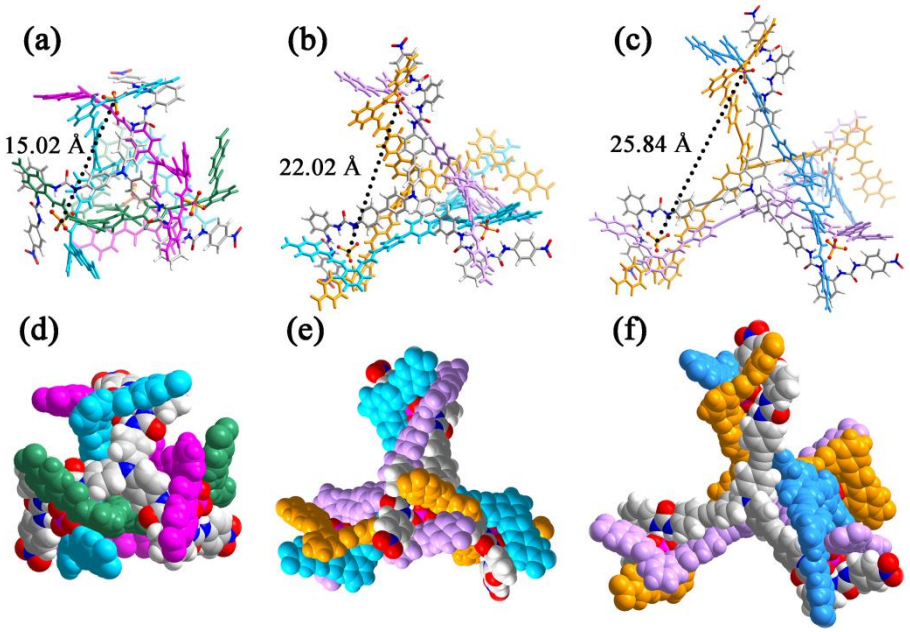

Fig. S56. Optimized structures of the tetrahedral complexes: (a) $[(PO_4)_4(\mathbf{L^1})_4]^{12-}$; (b) $[(PO_4)_4(\mathbf{L^2})_4]^{12-}$; (c) $[(PO_4)_4(\mathbf{L^3})_4]^{12-}$; and space-filling representations: (d) $[(PO_4)_4(\mathbf{L^1})_4]^{12-}$; (e) $[(PO_4)_4(\mathbf{L^2})_4]^{12-}$; (f) $[(PO_4)_4(\mathbf{L^3})_4]^{12-}$. Only a ΔΔΔΔ enantiomer is shown.

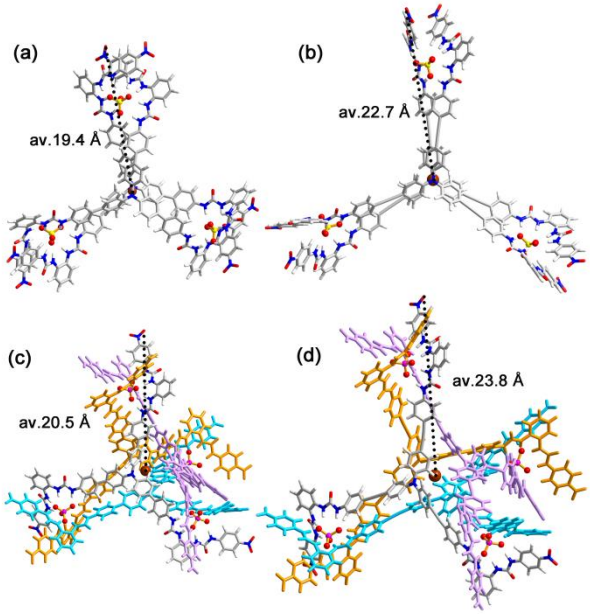

Fig. S57. Measured radius of the assemblies in the DFT-optimized structures: (a) $[(SO_4)_3(\mathbf{L^2})_2]^{6-}$; (b) $[(SO_4)_3(\mathbf{L^3})_2]^{6-}$; (c) $[(PO_4)_4(\mathbf{L^2})_4]^{12-}$; (d) $[(PO_4)_4(\mathbf{L^3})_4]^{12-}$.

S6. Volume calculations

A virtual probe with the minimum radius such that it would not exit the cavity of the largest structure was employed. The cavity volume of $[(PO_4)_4(\mathbf{L^1})_4]^{12-}$ is 77.07 $Å^3$ (1.4 Probe) (Figure S58). Because it was observed that the larger probe could not enter the host cavity during the calculation.

Primary grid spacing: 0.100

Maximum number of volume-refinement cycles: 30

Min size of secondary grid: 3

Grid for plot files: 0.100

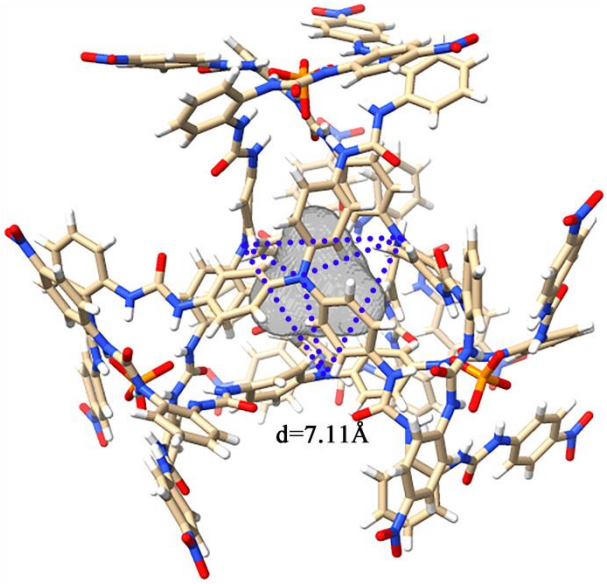

Fig. S58. Cavity surface (gray) of $[(PO_4)_4(\mathbf{L^1})_4]^{12-}$.

A virtual probe with the minimum radius such that it would not exit the cavity of the largest structure was employed. The cavity volume of the $[(\mathbf{L^2})_4(PO_4)_4]$ is 79.19 $Å^3$ (1.4 Probe, water-sized) (Fig. 59).

Primary grid spacing: 0.100

Maximum number of volume-refinement cycles: 30

Min size of secondary grid: 3

Grid for plot files: 0.100

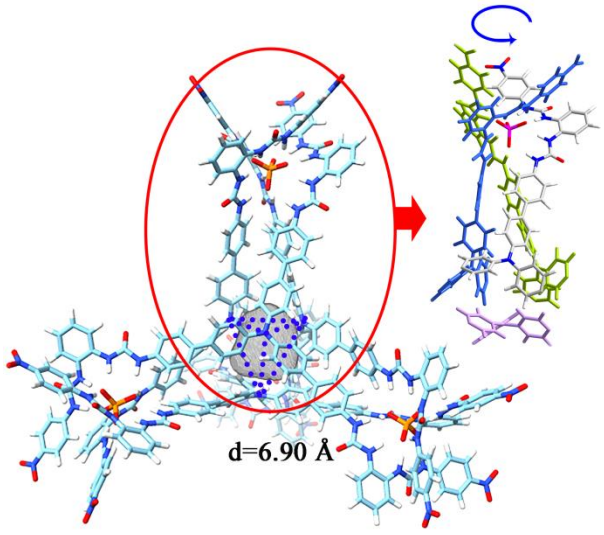

Fig. S59. Cavity surface (gray) of $[(PO_4)_4(\mathbf{L^2})_4]^{12-}$.

A virtual probe with the minimum radius such that it would not exit the cavity of the largest structure was employed. The cavity volume of the $[(\mathbf{L}^3)_4(PO_4)_4]$ is 68.38 $Å^3$ (1.4 Probe, water-sized) (Fig. S60).

Primary grid spacing: 0.100

Maximum number of volume-refinement cycles: 30

Min size of secondary grid: 3

Grid for plot files: 0.100

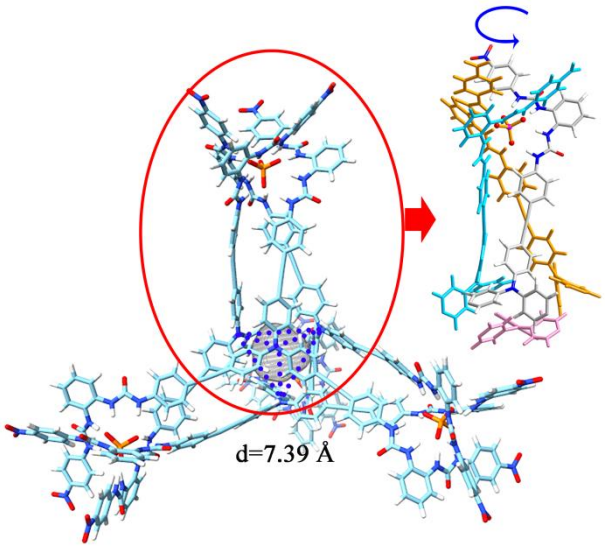

Fig. S60. Cavity surface (gray) of $[(PO_4)_4(\mathbf{L}^3)_4]^{12-}$.

S7. Supporting references

1 B. Wu, F. Cui, Y. Lei, S. Li, N. S. Amadeu, C. Janiak, Y.-J. Lin, L.-H. Weng, Y.-Y. Wang and X.-J. Yang, *Angew. Chem. Int. Ed*. 2013, **52**, 5096-5100.

2 J. G. Brandenburg, *J. Chem. Phys*. 2018, **148**, 064104-064117.

3 F. Neese, WIREs *Comput. Mol. Sci*. 2012, **2**, 73-78.

4 (a) S. Grimme, C. Bannwarth and P. Shushkov, *J. Chem. Theory Comput.* 2017, **13**, 1989-2009; (b) C. Bannwarth, S. Ehlert and S. Grimme, *J. Chem. Theory Comput.* 2019, **15**, 1652-1671.

5 xtb - An extended tight-binding semi-empirical program package, web site: http://grimme.unibonn.de/software/xtb.